Available online at www.sciencedirect.com

ScienceDirect

Geochimica et Cosmochimica Acta 238 (2018) 123–149

Geochimica et Cosmochimica Acta

www.elsevier.com/locate/gca

The theory of equilibrium isotope fractionations for gaseous molecules under super-cold conditions

Yining Zhang [a,b], Yun Liu [a,*]

[a] State Key Laboratory of Ore Deposit Geochemistry, Institute of Geochemistry, Chinese Academy of Sciences, Guiyang 550002, China
[b] University of Chinese Academy of Sciences, Beijing 100049, China

Received 28 February 2018; accepted in revised form 1 July 2018; available online 09 July 2018

Abstract

It is necessary to build a proper theoretical method that can precisely describe isotope fractionation processes under super-cold (<200 K) conditions, because there have been many isotopic data obtained in our solar system that are related to such processes. However, current methods of isotope fractionation calculation, i.e., the Bigeleisen-Mayer equation and its higher-order energy corrections, may not be applicable to super-cold conditions. Here, we have checked important assumptions and higher-order corrections that can affect isotope fractionations of gas-phase molecules under super-cold conditions and developed a new theoretical method for calculating equilibrium isotope fractionation factors. Compared with previous works, we have added three new corrections into our calculation, i.e., nuclear-spin weights for quantum mechanical rotation, correction for Born-Oppenheimer approximation (BOA), and inversion splitting effect for non-planar molecules such as NH_3. We further examined gaseous molecules of geochemistry and cosmochemistry relevance, e.g., H_2, HF, HCl, H_2O, H_2S, HCHO, NH_3, CH_4 and their deuterated isotopologues. We found that the correction for BOA, which was rarely considered in previous studies, is important for those gaseous molecules under super-cold conditions. In case of D/H, $^{13}C/^{12}C$ and $^{18}O/^{16}O$ exchanges among organic molecules, BOA correction cannot be ignored even at ambient or higher temperature conditions. Most isotope fractionation trends at super-cold conditions reported here are quite different from their counterparts at ambient or higher temperature conditions. The method proposed here will extend our capability in interpreting equilibrium isotope fractionations to super-cold conditions in the solar system.

1. INTRODUCTION

Urey (1947) and Bigeleisen and Mayer (1947) showed how to calculate equilibrium isotope fractionation factors with sufficient accuracy. Their methods were later referred to as the Urey model or the Bigeleisen-Mayer equation (hereafter B-M equation). The B-M equation can successfully predict equilibrium isotope fractionations at ambient and higher temperatures by only employing harmonic vibration frequencies of studied compounds. However, B-M equation has adopted a few approximations, notably those that are not adequate for super-cold conditions (<200 K) or H/D exchange reactions. With the progress in planetary sciences and space exploration, more and more isotopic data have been obtained for systems under extremely low temperatures (e.g., Pinto et al., 1986; Eberhardt et al., 1987; Robert et al., 2000; Cordier et al., 2008; Robert, 2010; Nixon et al., 2012; Webster et al., 2013; Altwegg et al., 2014). It is therefore necessary to examine and revise the approximations in B-M equation when it comes to super-cold conditions.

* Corresponding author.
E-mail address: liuyun@vip.gyig.ac.cn (Y. Liu).

https://doi.org/10.1016/j.gca.2018.07.001
0016-7037/

There are many corrections that have been proposed to improve the B-M equation since 1947, e.g., vibrational anharmonicity (including the G_0 term), quantum mechanical rotation, centrifugal distortion, vibration–rotation coupling, inversion splitting, and hindered internal rotator (e.g., Urey, 1947; Bigeleisen and Mayer, 1947; Wolfsberg, 1969a, 1969b; Wolfsberg et al., 1970; Born and Wolfsberg, 1972; Richet et al., 1977; Liu et al., 2010). All these corrections are related to translational, vibrational and rotational energy differences between isotopologues. In addition, the electronic energy difference has also been found to bring minor contributions to isotope fractionation. For example, Kleinman and Wolfsberg (1973) firstly pointed out the importance of electronic energy difference beyond the Born-Oppenheimer approximation (BOA) for isotopic exchange reactions. They found that this energy difference would cause significant fractionations for the HX + HD = DX + H_2 isotope exchange reaction from 1.029 (X = Li) to 1.101 (X = B) at 300 K. And this energy correction for other systems has also been evaluated, e.g., HCl (Postma et al., 1988); H + H_2 reaction (Mielke et al., 2005); CH_4 + C_2H reaction (Nixon et al., 2012); N_2 (Chakraborty et al., 2014); and Li_2, LiK, LiRb, Sr_2, Yb_2 (Lutz and Hutson, 2016). In 1989, another electronic energy isotope effect, the nuclear field shift or the nuclear volume effect (NVE), which is the electronic energy difference caused by different volumes and shapes of heavy metal isotopes was discovered (Fujii et al., 1989). Since then, many works have investigated the NVE both theoretically and experimentally (e.g., Bigeleisen, 1996; Nomura et al., 1996; Schauble, 2007, 2013; Fujii et al., 2009; Yang and Liu, 2015, 2016). In addition, nuclear-spin induced hyperfine splitting or symmetric splitting was found to cause minor fractionations for very heavy atoms (Bigeleisen, 1996). However, all these mentioned corrections on the B-M equation have only been examined for systems at >200 K conditions. The applicability of these corrections under super-cold conditions was entirely unknown.

Here we firstly reevaluate the approximations used in the B-M equation to test if they should be included into the calculation for super-cold conditions. Then, following the works of Richet et al. (1977) and Liu et al. (2010), we develop a method to calculate equilibrium isotope fractionation factors under super-cold conditions. This theoretical method includes important treatments on higher-level energy terms, such as vibrational anharmonicity (including G_0 term), quantum mechanical rotation (including nuclear-spin weights for molecules with different symmetries except the asymmetric-tops), centrifugal distortion, vibration-rotational coupling, inversion splitting (for NH_3 and its isotopologues), and the energy correction on BOA. Compared with previous studies, the nuclear-spin weights for quantum mechanical rotation, the correction on BOA, and the inversion splitting effect are three new corrections added here. We could but did not include the NVE into our calculation because NVE is significant only for heavy elements (generally Z > 40) and our systems are all light elements (e.g., H, C, N, O and S).

After systematic evaluation, we find that departures from the assumptions underlying the BOA introduce significant corrections to the systems we studied.

2. THEORY

2.1. The Urey model or the B-M equation

The B-M equation or the Urey model (Bigeleisen and Mayer, 1947; Urey, 1947) is the basis of calculating equilibrium isotope fractionation factors, and can be derived as follows.

For an isotopic exchange reaction as

$$AX_L + BX_H = AX_H + BX_L \tag{1}$$

where X_L and X_H denotes the light and heavy isotopes, respectively. Under statistical mechanical treatments, its equilibrium constant K_{eq} can be expressed by the ratio of partition functions:

$$K_{eq} = \frac{[AX_H]}{[AX_L]} / \frac{[BX_H]}{[BX_L]} = \frac{Q_{AX_H}}{Q_{AX_L}} / \frac{Q_{BX_H}}{Q_{BX_L}} = \frac{(Q_{trans}Q_{rot}Q_{vib})_{AX_H}}{(Q_{trans}Q_{rot}Q_{vib})_{AX_L}} / \frac{(Q_{trans}Q_{rot}Q_{vib})_{BX_H}}{(Q_{trans}Q_{rot}Q_{vib})_{BX_L}} \tag{2}$$

The terms Q_{trans}, Q_{rot} and Q_{vib} are the translational, rotational and vibrational partition functions, respectively. A partition function Q can be defined as

$$Q = \sum_i g_i \exp\left(-\frac{E_i}{k_B T}\right) \tag{3}$$

where E_i is the energy of the ith energy level with a degeneracy of g_i, k_B is the Boltzmann constant and T is the temperature in Kelvin.

Urey (1947) and Bigeleisen and Mayer (1947) used the harmonic oscillator and rigid rotator approximations to describe the motion of a molecule and ignored the electronic energy difference and other quantum effects for simplicity. Under these approximations, the expressions of Q_{trans}, Q_{rot} and Q_{vib} can then be easily given as follows (take a non-linear polyatomic molecule contains N atoms as example)

$$Q_{trans} = V\left(\frac{2\pi M k_B T}{h^2}\right)^{\frac{3}{2}} \tag{4}$$

$$Q_{rot} = \frac{\pi^{\frac{1}{2}}(8\pi^2 k_B T)^{\frac{3}{2}}(I_A I_B I_C)^{\frac{1}{2}}}{\sigma h^3} \tag{5}$$

$$Q_{vib} = \prod_{i=1}^{3N-6} \frac{\exp(-\frac{u_i}{2})}{1-\exp(-u_i)} \qquad u_i = \frac{hc\omega_i}{k_B T} \tag{6}$$

where V is volume, M is the molecular mass, I_A, I_B and I_C are the moment of inertia around axis A, B and C of rotation, h is the Planck constant, c is the speed of light in vacuum, σ is the symmetry number (the number of different but indistinguishable arrangements of a molecule; e.g., $\sigma(H_2) = 2$, $\sigma(HD) = 1$, $\sigma(H_2O) = 2$ and $\sigma(CH_4) = 12$) of the molecule and ω is the harmonic vibration frequency.

Bigeleisen and Mayer (1947) additionally employed the Teller-Redlich theorem or the isotope product rule (Redlich, 1935; Wilson et al., 1955) given by:

$$\frac{(I_A I_B I_C)^{\frac{1}{2}}_{AX_H}}{(I_A I_B I_C)^{\frac{1}{2}}_{AX_L}} \left(\frac{M_{AX_H}}{M_{AX_L}}\right)^{\frac{3}{2}} = \left(\frac{m_H}{m_L}\right)^{\frac{3n}{2}} \prod_{i=1}^{3N-6} \frac{u_{i,AX_H}}{u_{i,AX_L}} \tag{7}$$

where n is the number of X atoms been substituted (in this study, $n = 1$) and m_H, m_L is the mass of the X_H and X_L atoms. The B-M equation is thus given by inserting Eqs. (4)-(6) into Eq. (2) and applying Eq. (7):

$$\frac{Q_{AX_H}}{Q_{AX_L}} = \frac{\sigma_{AX_L}}{\sigma_{AX_H}}\left(\frac{m_H}{m_L}\right)^{\frac{3}{2}} \times \prod_{i=1}^{3N-6}\left[\frac{u_{i,AX_H}}{u_{i,AX_L}}\frac{\exp\left(-\frac{u_{i,AX_H}}{2}\right)}{\exp\left(-\frac{u_{i,AX_L}}{2}\right)}\frac{1-\exp(-u_{i,AX_L})}{1-\exp(-u_{i,AX_H})}\right] \quad (8)$$

where the $\frac{\sigma_{AX_H}}{\sigma_{AX_L}}\frac{Q_{AX_H}}{Q_{AX_L}}/\left(\frac{m_H}{m_L}\right)^{\frac{3}{2}}$ term is called the reduced partition function ratio (RPFR) of the isotopologue pair AX_H/AX_L (Bigeleisen and Mayer, 1947). Thus, the RPFR can be expressed as

$$RPFR(AX_H/AX_L) = \prod_{i=1}^{3N-6}\frac{u_{i,AX_H}}{u_{i,AX_L}}\frac{\exp\left(-\frac{u_{i,AX_H}}{2}\right)}{\exp\left(-\frac{u_{i,AX_L}}{2}\right)} \times \frac{1-\exp(-u_{i,AX_L})}{1-\exp(-u_{i,AX_H})} \quad (9)$$

The equilibrium fractionation factor α is equal to K_{eq} for a single-isotope-substitution reaction between AX and BX. At the B-M equation theoretical treatment level, α is equal to the ratio of two RPFRs:

$$K_{eq} = \alpha_{AX-BX} = \frac{RPFR(AX_H/AX_L)}{RPFR(BX_H/BX_L)} \quad (10)$$

Theorists often use the β factor (Schauble, 2004), which is a special isotope fractionation factor between a compound and ideal mono-atomic gas of the interested isotope system, e.g., between water and mono-atomic O gas if O isotope is the interested isotope system. The β factor shows the ability of heavy isotope enrichment of a certain compound. The relation between β factor and fractionation factor α is

$$\beta_{AX} = \alpha_{AX-X} \quad (11)$$

Therefore, the isotope fractionation factor α between AX and BX is the ratio of two β factors (Note that only at the B-M equation treatment level, β factor is equal to RPFR.):

$$\alpha_{AX-BX} = \frac{\beta_{AX}}{\beta_{BX}} \quad (12)$$

2.2. Approximations or assumptions used in the B-M equation

Here we review the assumptions that underlie the B-M equation and check whether they are still valid under low temperature conditions or not. The approximations or assumptions used in the B-M equation are:

(a) The gaseous systems must be ideal so that the pressure-volume work difference can be ignored.
(b) The systems are dilute and particles can be distinguished from one another. As a result, the translational motions of the molecule are assumed to obey the *Maxwell-Boltzmann-Statistics* (MBS). To check the validity of this assumption, we can use the common threshold $\frac{N}{V}\left(\frac{h^2}{2\pi M k_B T}\right)^{\frac{3}{2}} << 1$, where N and V are the number of molecules and the volume of the system, respectively. After simple calculation, we find that all the gaseous molecules used in this study perfectly satisfy this requirement (more details can be find in Supplementary file, Section S1).
(c) Q_{trans} can be calculated with an analytic expression rather than direct summation. The translational motion of a molecule can be described by 3 quantum number n_x, n_y and n_z after solving the 3-dimensional Schrödinger equation in a cubic box with an edge of l. The energy levels can be expressed as follows:

$$E(n_x, n_y, n_z) = \frac{h^2}{8Ml^2}\left({n_x}^2 + {n_y}^2 + {n_z}^2\right) \quad (13)$$

When the system is at ambient conditions, the interval between two neighboring translational energy states is very small. The triple summation hence can be approximated into a product of three independent integrations:

$$Q_{trans} = \sum_{n_x}^{+\infty}\sum_{n_y}^{+\infty}\sum_{n_z}^{+\infty}\exp\left[-\frac{h^2}{8Ml^2k_BT}\left({n_x}^2 + {n_y}^2 + {n_z}^2\right)\right] \approx \left[\int_0^{+\infty}\exp\left(-\frac{h^2n^2dn}{8Ml^2k_BT}\right)\right]^3 = l^3\left(\frac{2\pi Mk_BT}{h^2}\right)^{\frac{3}{2}} = \left(\frac{2\pi Mk_BT}{h^2}\right)^{\frac{3}{2}}V \quad (14)$$

However, when the temperature decreases, the summation interval increases exponentially. Therefore, we need to check whether it is reasonable to use the integration treatment under super-cold conditions or not. Fortunately, due to the extremely small value of $\frac{h^2}{8Ml^2k_BT}$ for ideal gases under super-cold conditions, i.e., the common average value is $\sim 10^{-16}$, when M is 2 g mol^{-1} (corresponding to 3.32×10^{-27} kg), T is 20 K and l is 1 cm. It is still appropriate for using the integration approximation treatment.

(d) Rotational motion of a molecule is rigid and Q_{rot} can be calculated by integration rather than summation. For most molecules, their rotational temperatures ($\Theta = \frac{h^2}{8\pi^2 I k_B}$, generally < 10 K) can be ignored when compared with the system temperature T ($\frac{\Theta}{T} \to 0$), therefore Q_{rot} can be easily calculated by (such as for a diatomic molecule):

$$Q_{rot} = \sum_{J=0}^{+\infty}(2J+1)\exp\left[-\frac{\Theta}{T}J(J+1)\right] \approx \int_0^{+\infty}\exp\left(-\frac{\Theta}{T}x\right)dx = \frac{T}{\Theta} \quad (15)$$

Here the $(2J + 1)$ term in front of the exponent is the degeneracy of the Jth rotational energy level. However, when Θ is very high or the system temperature is low, we cannot directly use this approximation to calculate Q_{rot},

especially for H_2 (e.g., Bigeleisen and Mayer, 1947; Richet et al., 1977). In addition, the nuclear-spin effect due to the nuclear-spin statistics will become significant at low temperatures (e.g., Fox, 1970; McDowell, 1987, 1988, 1990; Arrighini and Guidotti, 1995), and the effects of centrifugal distortion and vibration-rotational coupling should be considered, too. Although it is often believed that the later two effects are important at high temperatures (Richet et al., 1977; Liu et al., 2010), we still need to check them at low temperatures to ensure whether they can be safely ruled out or not. Therefore, the calculation method of Q_{rot} should be revised under super-cold conditions.

(e) Harmonic oscillator approximation. Vibrational anharmonicity correction has been shown to be very important for calculating isotope fractionations by many studies (e.g., Wolfsberg, 1969a, 1969b; Wolfsberg et al., 1970; Born and Wolfsberg, 1972; Richet et al., 1977; Bigeleisen, 1996; Liu et al., 2010). Hence it is important to take this correction into account.

(f) The Born-Oppenheimer approximation (BOA). The BOA assumes that the motion of electron and nuclei of a molecule can be treated independently (actually they are coupled), therefore the electronic energy of a molecule and all its isotopologues are exactly the same. Actually, when we consider the electronic energy of a molecule beyond the BOA, the coupling between the motion of electrons and nuclei must be included, which corresponds to an energy correction for the BOA. As early as in 1973, researchers had pointed out that the energy corrections for the BOA had unexpected large effect for H/D isotope fractionation factors even at 300 K (Kleinman and Wolfsberg, 1973). Bigeleisen (1996) also suggested the necessity of considering this effect. However, this correction has not been seriously considered by most of studies due to its difficulty of computation. Therefore, this correction should be systematically checked for both equilibrium and kinetic isotope fractionation processes.

2.3. Quantum mechanical rotation with nuclear-spin weights for a rigid rotator

In the effort to re-derive a framework for describing isotope fractionation factors under super-cold conditions, we will begin with describing a comprehensive way to calculate the Q_{rot} of a molecule.

Typically, a molecule is regarded as a rigid rotator and its Q_{rot} can be calculated using Eq. (5) or Eq. (15). However, at low temperatures, the interval between two neighboring rotational energy states is too wide to use the integration approximation. A direct summation method must be employed. However, even direct summation cannot give the precise value of Q_{rot} at low temperatures due to the nuclear-spin statistics restrictions (e.g., Herzberg, 1945; Fox, 1970; McDowell, 1987, 1988, 1990). For a molecule with a specific symmetry, when two of its identical atoms are interchanged, its wavefunction must satisfy interchange symmetry restrictions, i.e., its wavefunction must be antisymmetric or symmetric, as a result of Pauli exclusion theorem. This restriction leads to different nuclear-spin weights for the rotational energy levels so that the calculated Q_{rot} will significantly deviates from the typical one. Previous studies showed that this deviation became significant at low temperatures and rapidly vanished as the temperature increasing (e.g., Fox, 1970; McDowell, 1987, 1988, 1990). Therefore, precise Q_{rot} must be calculated with the consideration of nuclear-spin weights under super-cold conditions. In addition, all spin isomers of the molecule must also be in thermodynamic equilibrium to guarantee the use of nuclear-spin weights. The disequilibrium issue will be simply discussed in Section 5.6.

Because different symmetries of molecule will lead to different nuclear-spin weights, we separate them into 4 types according to their symmetry and three rotational constants along the principal rotation axis:

(1) Linear molecules (including diatomic molecules)

If without a center of symmetry (e.g., HD, HCN), all nuclear spin weights are the same and Q_{rot} can be directly summated using Eq. (15). If with a center of symmetry (e.g., H_2, CO_2), there are different nuclear spin weights and Q_{rot} should be directly summed with such weights.

We denote a linear molecule with a center of symmetry as *L-L* (e.g., H_2, C_2H_2) or *L-X-L* (e.g., CO_2), which *L* is one of the two identical ligands or atoms. Thus the nuclear-spin weights of each rotational level can be written as

$$J = even : \frac{1}{2} I(I - \kappa) \tag{16}$$

$$J = odd : \frac{1}{2} I(I + \kappa) \tag{17}$$

where J is the rotation quantum number (0, 1, 2, 3…), I is the total nuclear-spin multiplicity of ligand L and it equals to the product of the nuclear-spin multiplicity of all atoms in L. The nuclear-spin multiplicity of an atom is $2I_X + 1$, and I_X is the nuclear spin of atom X. If the sum of nuclear spin for all atoms in ligand L is half-integer (1/2, 3/2, 5/2, 7/2…), then the κ is -1, i.e., H_2. If the sum is an integer (0, 1, 2, 3…), then κ is $+1$, i.e., D_2 or CO_2 (Herzberg, 1945; McDowell, 1988; Arrighini and Guidotti, 1995). Therefore, the complete expression of Q_{rot} is

$$\begin{aligned} Q_{rot} = {} & \tfrac{1}{2} I(I + \kappa) \sum_{J=0,2,4\ldots}^{+\infty} (2J+1) \exp\left[-J(J+1)\tfrac{hcB}{k_B T}\right] \\ & + \tfrac{1}{2} I(I - \kappa) \sum_{J=1,3,5\ldots}^{+\infty} (2J+1) \exp\left[-J(J+1)\tfrac{hcB}{k_B T}\right] \end{aligned} \tag{18}$$

where B is the rotational constant defined as $B = \frac{h}{8\pi^2 c I_B}$, which is one of the two identical rotational constants for a linear molecule. To avoid confusion when calculating the Q_{rot} ratio due to the symmetry number and nuclear spin multiplicity, the Q_{rot} must be normalized. Taking the H_2 and D_2 as examples, their nuclear spin weights are 1, 3 and 6, 3 for the even and odd rotational energy levels, which

correspond to a total multiplicity of 4 and 9. As a result, the Q_{rot} of D_2 will be scaled by a factor of 2.25 (9/4) relative to the Q_{rot} of H_2 if we directly use the Eq. (18) without normalization, which causes unnecessary confusion in the calculation of the final Q_{rot} ratio. It is the reason why the Q_{rot} including the nuclear spin weights must be normalized. Here we import the normalization factor $1/N$ that equals $\frac{\sigma}{I^2}$ for linear molecules we discussed here, and the denominator is the sum of all nuclear-spin weights, which equals I^2 for a linear molecule we discussed here. For example, for H_2, D_2 and CO_2, $1/N$ equals to 1/2, 2/9 and 2, respectively.

(2) Spherical top molecules

For a spherical top molecule like methane (CH_4), if we don't take the nuclear-spin effects into account, we can calculate its Q_{rot} by using the following formula:

$$Q_{rot} = \frac{1}{12}\sum_{J=0}^{+\infty}(2J+1)^2\exp\left[-J(J+1)\frac{hcB}{k_BT}\right] \tag{19}$$

where spherical-tops have a $(2J+1)^2$ rather than $(2J+1)$ degeneracy for each energy level, and 12 is the symmetry number.

The nuclear-spin weights of a spherical top molecule will become much more complicated than the linear molecules due to its high symmetry. Fox (1970) and McDowell (1987) evaluated the nuclear-spin weights for CH_4 at low temperatures. Their formula can be summarized as

$$\begin{aligned} Q_{rot} = {} & \frac{(2I_H+1)^4}{12}\sum_{J=0}^{+\infty}(2J+1)^2\exp\left[-J(J+1)\frac{hcB}{k_BT}\right] \\ & + \frac{(2I_H+1)^2}{4}\sum_{J=0}^{+\infty}(-1)^J(2J+1)\exp\left[-J(J+1)\frac{hcB}{k_BT}\right] \\ & + \frac{4(2I_H+1)^2}{3\sqrt{3}}\sum_{J=0}^{+\infty}(2J+1)\left[\sin\frac{(2J+1)\pi}{3}\right]\exp\left[-J(J+1)\frac{hcB}{k_BT}\right] \end{aligned} \tag{20}$$

where I_H is the nuclear spin of H atom, which is 1/2. Also, the normalization factor $1/N$ for a methane-like molecule (XY_4) equals $\frac{\sigma}{(2I_Y+1)^4}$, which is 3/4 (= 12/16) for CH_4 and 4/27 (= 12/81) for CD_4.

(3) Symmetric top molecules

For a symmetric top molecule like NH_3 or CH_3D, they can be described as WX_3 or WXY_3, and they exhibit two sub-types of symmetries. One is the prolate top and the other is the oblate top, which differs in their rotational constants. If their rotational constants A, B and C satisfy the conditions of $B = C$ and $A > B$, then it is a prolate top (such as CH_3D); If their rotational constants satisfy $A = B$ and $B > C$, then it is an oblate top (such as NH_3). The Q_{rot} of a prolate top molecule can be calculated without nuclear-spin weights by

$$\begin{aligned} Q_{rot} = {} & \sum_{J=0}^{+\infty}(2J+1)\exp\left[-J(J+1)\frac{hcB}{k_BT}\right] \\ & \times\sum_{K=-J}^{J}\exp\left[-\frac{hc(A-B)}{k_BT}K^2\right] \end{aligned} \tag{21}$$

If it is for oblate tops, A should be replaced by C in the above equation (McDowell, 1990).

If with the nuclear-spin weights, Q_{rot} can be calculated by

$$\begin{aligned} Q_{rot} = {} & \sum_{J=0}^{+\infty}(2J+1)\exp\left[-J(J+1)\frac{hcB}{k_BT}\right] \\ & \times\sum_{K=-J}^{J}g(K)\exp\left[-\frac{hc(A-B)}{k_BT}K^2\right] \end{aligned} \tag{22}$$

where $g(K)$ is

$$g(K) = \frac{(2I+1)^3}{3}\left[1+\frac{2}{(2I+1)^2}\cos\left(\frac{2\pi K}{3}\right)\right] \tag{23}$$

where I is the nuclear spin of one of the three identical atoms and the normalization factor $1/N$ equals to $\frac{3}{(2I+1)^3}$, which is 3/8 for NH_3 and CH_3D.

(4) Asymmetric top molecules

The Q_{rot} of an asymmetric-top molecule with the nuclear-spin weights can be calculated by the following formula:

$$Q_{rot} = \sum_{J,K_a,K_c}^{+\infty}(2J+1)g(K_a,K_c)\exp\left[-\frac{E(J,K_a,K_c)}{k_BT}\right] \tag{24}$$

However, the exact analytic expression of $E(J, K_a, K_c)$ is unknown, which means it is impossible for us to directly calculate Q_{rot} except solving the rotational Hamiltonian for each J-level individually through numerical method (Dennison and Hecht, 1962). So a precise Q_{rot} must be calculated by direct summing up thousands of the rotational energy levels measured by experiments or calculated by high-accuracy quantum calculations. Fortunately, Watson (1988) derived a high-temperature asymptotic formula, which has been tested to be accurate enough and comparable with the precise value by direct summing of the experimental measures within 0.5%.

We used $H_2^{16}O$, $HD^{16}O$ and $H_2^{32}S$ for the testing. $H_2^{16}O$ and $H_2^{32}S$ have a C_2 rotating axis which means their two identical H atoms must satisfy the interchange symmetry restriction. $H_2^{16}O$ and $H_2^{32}S$ hence have the same nuclear-spin weights, which are 3 and 1 when the rotational quantum number $(K_a + K_c)$ is odd or even (Tennyson et al., 2001). Then the accurate Q_{rot} for $H_2^{16}O$ or $H_2^{32}S$ can be calculated using the measured rotational lines at its ground vibrational state:

$$\begin{aligned} Q_{rot}(H_2O) = {} & \frac{3}{2}\sum_{K_a+K_c=\ odd}^{+\infty}(2J+1)\exp\left[-\frac{E(J,K_a,K_c)}{k_BT}\right] \\ & +\frac{1}{2}\sum_{K_a+K_c=\ even}^{+\infty}(2J+1)\exp\left[-\frac{E(J,K_a,K_c)}{k_BT}\right] \end{aligned} \tag{25}$$

where 1/2 is for normalization.

For HDO, there are no identical atoms, meaning all the nuclear-spin weights are the same and its Q_{rot} can be directly summed. For H_2O, HDO and H_2S, the contributions of the rotational lines at excited vibrational states can be approximated using the equation $\exp\left(-\frac{hc\upsilon_{\min}}{k_BT}\right)$ where the $\upsilon_{\min}$ is the

smallest vibrational fundamental. After a simple calculation, this contribution is very small and can be safely ignored (H_2O: 0.05%; HDO: 0.13%; H_2S: 0.32%; $T = 300$ K).

The following equation is the asymptotic formula for calculating Q_{rot} without considering nuclear-spin weights (Watson, 1988):

$$Q_{rot} = \left(\frac{\pi}{abc}\right)^{\frac{1}{2}} e^{f_1}(1 + f_2 + f_3) \tag{26}$$

where

$$f_1 = \frac{1}{12}\left[2\sum a - \sum \frac{ab}{c}\right] \tag{27}$$

$$f_2 = \frac{1}{90}\sum \frac{ab(c-a)(c-b)}{c^2} \tag{28}$$

$$f_3 = \frac{1}{2835} \times \sum \frac{(c-a)(c-b)}{c^3}\left[(a-b)^2c^2 + 4(a+b)abc - 8a^2b^2\right] \tag{29}$$

and a, b and c are dimensionless rotational constants $\frac{hcA}{k_BT}$, $\frac{hcB}{k_BT}$ and $\frac{hcC}{k_BT}$, respectively. The summation symbol means a rotational summation for a, b and c (e.g., $\sum a = a + b + c$ and $\sum \frac{ab}{c} = \frac{ab}{c} + \frac{bc}{a} + \frac{ca}{b}$).

Fig. 1 shows the Q_{rot} differences calculated using different methods. The Y-axis denotes the deviations of the calculated results using Eq. (26) to the ones calculated by direct summation in the unit of per mil (‰). First, the solid curves show the deviations of the Q_{rot} calculated using the Eq. (26) to the directly summed results for $H_2^{16}O$, $HD^{16}O$ and $H_2^{32}S$ by previous researchers. When temperature is higher than a critical value ($H_2^{16}O$: ~80 K; $HD^{16}O$: ~40 K; H_2S: ~50 K), the deviations increase linearly. However, when temperatures are lower than the critical values, the deviations increase rapidly. The increasing deviations with increasing temperature above the critical temperatures can be satisfactorily explained by centrifugal distortion effect. We have computed the centrifugal distortion effects (see Section 2.4 for details) and illustrated in Fig. 1 in terms of their contributions to the total deviation (Three dashed lines). Thus, if the centrifugal distortion effects are factored into the computation of the rotational partition functions (three solid lines), the deviations become essentially negligible above the critical temperatures. However, below the critical temperatures, centrifugal distortion effect is not adequate to explain those huge deviations. The effect arising from the nuclear-spin weights will significantly affect the result of the calculated Q_{rot}. For $H_2^{16}O$, the deviation between the calculated results and the direct summing of experimental measures are 13.3% at 20 K. For a heavier molecule as $H_2^{32}S$, i.e., with much smaller rotational constants, its nuclear-spin weight effect occurs at even lower temperatures (<40 K). However, for $HD^{16}O$, the increased deviation below ~40 K can only be explained by the failure of Eq. (26) at extremely low temperatures due to there is no nuclear-spin effect for $HD^{16}O$. In general, Eq. (26) will give us accurate results within 0.5% deviations through the ambient or high temperatures until 50 K (e.g., $HD^{16}O/H_2^{16}O$, green dashed curve). Lower than 50 K we must consider the nuclear-spin weight effect. In addition, Watson (1988) also tried to add an approximated term to his asymptotic equation to take the nuclear-spin effect into account. However, our testing results show that this approximated term gives worse results than the ones without it. Therefore, we would recommend to not including this term into the Q_{rot} calculation.

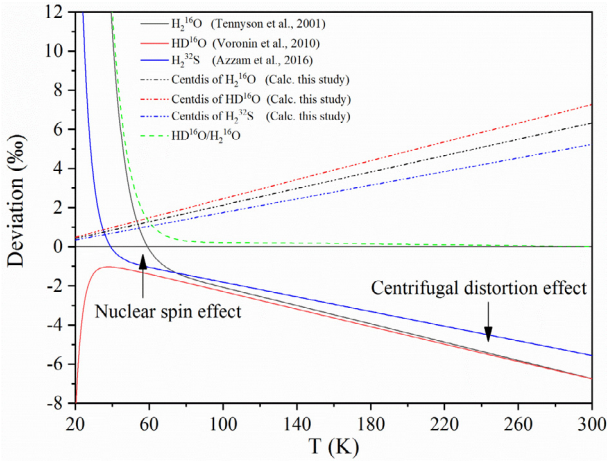

Fig. 1. Deviations between the direct summation of the experimentally measured or high-accuracy calculated rotational lines at the ground vibrational state and calculated by the formula of Watson (1988). The deviations were calculated by Deviation = [Q_{rot} (Calculated)/Q_{rot} (Summated) − 1] * 1000. $H_2^{16}O$; 1030 measured rotational lines (Tennyson et al., 2001) with $A = 28.0887\ cm^{-1}$, $B = 14.4453\ cm^{-1}$ and $C = 9.2490\ cm^{-1}$; $HD^{16}O$; 1625 calculated high-accuracy rotational lines (Voronin et al., 2010) with $A = 23.4140\ cm^{-1}$, $B = 9.1031\ cm^{-1}$ and $C = 6.4066\ cm^{-1}$; $H_2^{32}S$; 1704 calculated high-accuracy rotational lines (Azzam et al., 2016) with $A = 10.3466\ cm^{-1}$, $B = 9.0357\ cm^{-1}$ and $C = 4.7268\ cm^{-1}$. The Centdis means the deviation caused by centrifugal distortion effect, which equals (f_c − 1) * 1000 and f_c was obtained through the calculated molecular constants at MP2/aug-cc-pVTZ level.

2.4. Centrifugal distortion

A molecule will never be an ideal rigid rotator in the real world, which leads to a minor deviation of Q_{rot} from that of rigid-rotator, especially at high temperatures. As a result, Q_{rot} calculated using a rigid rotator model is always smaller than the one based on a non-rigid model (See Fig. 1). This deviation is caused by the centrifugal distortion effect. Previous studies have evaluated this effect on isotope fractionation at ambient and high temperature conditions (Richet et al., 1977; Liu et al., 2010) but it remains unclear whether this effect is important at much lower temperatures.

Previous studies have quantitatively evaluated this effect for different type of molecules (e.g., Wilson, 1936; Kivelson and Wilson, 1952; McDowell, 1987, 1988, 1990; Martin et al., 1991). For the 4 types of molecules considered here (linear, spherical-tops, symmetric-tops and asymmetric-tops), accurate formulas to describe the centrifugal distortion were derived by importing a simple correction factor f_c:

(a). Linear molecules (McDowell, 1988; Martin et al., 1991):

$$E_r = BJ(J+1) - DJ^2(J+1)^2 + HJ^3(J+1)^3 \quad (30)$$

$$f_c = 1 + \frac{2d(3-\beta)}{3\beta} + \frac{6(2d^2-h)}{\beta^2} + \frac{120d(d^2-h)}{\beta^3} \quad (31)$$

where B, D and H are rotational constant, quartic and sextic centrifugal constants in the unit of cm^{-1}, and β, d and h are dimensionless constants expressed as $\frac{hcB}{k_BT}$, D/B and H/B, respectively.

(b). Spherical-tops (McDowell, 1987):

$$E_r = BJ(J+1) - DJ^2(J+1)^2 + HJ^3(J+1)^3 \quad (32)$$

$$f_c = 1 + \frac{15d}{4\beta} \text{ or } 1 + \frac{3d(5-\beta)}{4\beta} + \frac{105(9d^2-4h)}{32\beta^2} + \frac{3465d(13d^2-12h)}{128\beta^3} \quad (33)$$

(c). Symmetric-tops (McDowell, 1990; Martin et al., 1991):

$$\begin{aligned} E_r = {} & BJ(J+1) + (A-B)K^2 - D_JJ^2(J+1)^2 \\ & - D_{JK}J(J+1)K^2 - D_KK^4 + H_JJ^3(J+1)^3 \\ & + H_{JK}J^2(J+1)^2K^2 + H_{KJ}J(J+1)K^4 + H_KK^6 \end{aligned} \quad (34)$$

Here D_J, D_{JK} and D_{KJ} are quartic centrifugal constants, and H_J, H_{JK}, H_{KJ} and H_K are sextic centrifugal constants. The expression of f_c for symmetric-tops is cumbersome. Please see Supplementary file Eqs. (S1)–(S5) for details.

Supplementary data associated with this article can be found, in the online version, at https://doi.org/10.1016/j.gca.2018.07.001.

(d). Asymmetric-tops (Martin et al., 1991):

The rotational Hamiltonian (Watson, 1968) for an asymmetric-top molecule is

$$\hat{H} = \hat{H}_2 + \hat{H}_4 + \hat{H}_6 \quad (35)$$

with

$$\hat{H}_2 = XJ_x^2 + YJ_y^2 + ZJ_z^2 \quad (36)$$

$$\begin{aligned} \hat{H}_4 = {} & T_{xx}J_x^4 + T_{yy}J_y^4 + T_{zz}J_z^4 + T_{xy}(J_x^2J_y^2 + J_y^2J_x^2) \\ & + T_{yz}(J_y^2J_z^2 + J_z^2J_y^2) + T_{zx}(J_z^2J_x^2 + J_x^2J_z^2) \end{aligned} \quad (37)$$

$$\begin{aligned} \hat{H}_6 = {} & \Phi_{xxx}J_x^6 + \Phi_{yyy}J_y^6 + \Phi_{zzz}J_z^6 + \Phi_{xxy}(J_x^4J_y^2 + J_y^2J_x^4) \\ & + \Phi_{xxz}(J_x^4J_z^2 + J_z^2J_x^4) + \Phi_{yyz}(J_y^4J_z^2 + J_z^2J_y^4) \\ & + \Phi_{yyx}(J_y^4J_x^2 + J_x^2J_y^4) + \Phi_{zzx}(J_z^4J_x^2 + J_x^2J_z^4) \\ & + \Phi_{zzy}(J_z^4J_y^2 + J_y^2J_z^4) + \Phi_{xyz}(J_x^2J_y^2J_z^2 + J_z^2J_y^2J_x^2) \end{aligned} \quad (38)$$

where T and Φ are quartic and sextic centrifugal constants. The expression of f_c is lengthy (see Supplementary file Eqs. (S6)–(S13)).

2.5. Vibrational anharmonicity

Vibrational anharmonicity has been shown to be an important factor in the computation of accurate equilibrium fractionation factors (e.g., Wolfsberg, 1969a, 1969b; Wolfsberg et al., 1970; Richet et al., 1977; Liu et al., 2010). Under the framework of second-order perturbation theory, the vibrational energy level of a polyatomic molecule is

$$\frac{E}{hc} = G_0 + \sum_i \omega_i\left(n_i + \frac{d_i}{2}\right) + \sum_{i=1} \times \sum_{j\geqslant i} x_{ij}\left(n_i + \frac{d_i}{2}\right)\left(n_j + \frac{d_j}{2}\right) + \sum_{s\geqslant t} g_{st}l_sl_t \quad (39)$$

where G_0 is an anharmonic term in the unit of cm^{-1}, which is the direct result of the perturbation theory and vanishes in actual spectroscopic measurements. The subscripts s and t denotes doubly-degenerated vibrational modes, ω_i and d_i are harmonic frequency and degeneracy of the ith vibration mode, x_{ij} is the anharmonic constants and the g_{st} is the anharmonic constant of vibrational l-doubling (Only for HCN, DCN in this study) in the unit of cm^{-1}. To calculate G_0 term, many researchers had derived different formulas (e.g., Shaffer, 1941; Shaffer and Schuman, 1944; Wolfsberg, 1969a, 1969b; Born and Wolfsberg, 1972; Bron, 1974; Pliva, 1990; Truhlar and Isaacson, 1991; Cohen et al., 1992; Zhang et al., 1993; Barone and Minichino, 1995; Barone, 2004, 2005; Willetts and Handy, 1995; Isaacson, 2002, 2006; Tajti et al., 2004; Schuurman et al., 2005; Bomble et al., 2006; Vázquez and Stanton, 2006; Pfeiffer et al., 2013; Piccardo et al., 2015). Here we use three different formulas to calculate G_0 term for molecules with different symmetries.

For diatomic molecules (e.g., H_2), the vibrational energy levels can be written as

$$\frac{E_n}{hc} = G_0 + \omega_e\left(n + \frac{1}{2}\right) - \omega_ex_e\left(n + \frac{1}{2}\right)^2 \quad (40)$$

where ω_e is the harmonic vibrational frequency with the unit of cm^{-1} and x_e is a dimensionless anharmonic term, which is always positive. Here G_0 can be expressed as (Wolfsberg, 1969b)

$$G_0 = \frac{B_e}{4} + \frac{\alpha_e\omega_e}{12B_e} + \frac{{\alpha_e}^2{\omega_e}^2}{144{B_e}^3} - \frac{\omega_ex_e}{4} \quad (41)$$

where B_e is the equilibrium rotational constant and α_e is the vibration-rotational coupling constant both with the unit of cm^{-1}.

For all the non-linear polyatomic molecules considered in this study, the expression for G_0 term can be summarized as (Born and Wolfsberg, 1972; Barone, 2004, 2005; Piccardo et al., 2015)

$$G_0 = \frac{1}{64}\sum_i \phi_{iiii} - \frac{7}{576}\sum_i \frac{\phi_{iii}^2}{\omega_i} + \frac{3}{64}\sum_{i\neq j} \frac{\omega_i\phi_{ijj}^2}{4\omega_j^2-\omega_i^2} - \frac{1}{4}\sum_{i<j<k} \frac{\omega_i\omega_j\omega_k\phi_{ijk}^2}{\Delta_{ijk}} - \frac{1}{4}\sum_{\alpha=x,y,z}\sum_{m<n} B_e^\alpha\left[1 + 2\left(\zeta_{mn}^\alpha\right)^2\right] \quad (42)$$

where ϕ_{iii} and ϕ_{iiii} are reduced cubic and quartic force constants in the unit of cm^{-1}, B_e^α is the equilibrium rotational constant along the principal rotation axis α, ζ_{mn}^α is the Coriolis coupling constant and Δ_{ijk} is defined as

$$\Delta_{ijk} = (\omega_i + \omega_j + \omega_k)(\omega_i + \omega_j - \omega_k)(\omega_i - \omega_j + \omega_k)(\omega_i - \omega_j - \omega_k) \quad (43)$$

For triatomic linear molecules in this study (HCN and DCN), we use the equation of Bron (1974) and Isaacson (2002) to calculate its G_0 term:

$$G_0 = \frac{1}{64}(\phi_{1111} + \phi_{2222}) + \frac{1}{48}\phi_{3333} - \frac{7}{576}\left(\frac{\phi_{111}^2}{\omega_1} + \frac{\phi_{222}^2}{\omega_2}\right) + \frac{3}{64}\left(\frac{\omega_2\phi_{211}^2}{4\omega_1^2-\omega_2^2} + \frac{\omega_1\phi_{221}^2}{4\omega_2^2-\omega_1^2}\right) + \frac{1}{16}\left(\frac{\omega_1\phi_{331}^2}{4\omega_3^2-\omega_1^2} + \frac{\omega_2\phi_{332}^2}{4\omega_3^2-\omega_2^2}\right) \quad (44)$$

where ω_3 is the doubly-degenerated vibrational mode.

Difficulties arise in the anharmonic treatment of vibrational energy levels under high-temperature conditions. For molecules at high temperatures (such as >1000 K), the value of the vibrational quantum number n becomes too large to get the correct vibrational frequencies and even negative frequencies instead due to flaws in perturbation theory. As a result, a numerical converging summation method must be developed to calculate Q_{vib} at high temperatures when the perturbation theory does not work sometimes (Truhlar and Isaacson, 1991).

In the present study we are dealing with systems under super-cold conditions, which means that almost all molecules are in the ground vibrational energy state and the contributions of excited states to Q_{vib} are very small and even can be ignored. To obtain Q_{vib}, we have summed up the first hundreds or thousands of excited vibrational energy states at anharmonic level, which corresponding to an n_m (the biggest vibrational quantum number) of 5 or 10. To determine the value of n_m that the value of Q_{vib} converged, we have calculated the Q_{vib} at 300 K by changing the value of n_m from 0 to 50. For convenience, we used the same n_m for each vibrational mode with a very tight convergence threshold ($\frac{Q_{vib}(n_m+1)}{Q_{vib}(n_m)} - 1 \leqslant 10^{-6}$). Our result shows that the corresponding values of n_m are small enough to guarantee the validity of the perturbation theory at temperatures lower than 300 K and all molecules considered here have been carefully checked without exception.

2.6. Vibration-rotation coupling

The vibrational and rotational motions of a molecule were treated independently in the classical Urey model or the B-M equation. However, the vibration and rotation of molecules are coupled in the real world. Therefore, the true rotational constants along the principal axis at different vibrational states are different, and can be expressed by (Pennington and Kobe, 1954; Barone, 2005)

$$B_n = B_e - \sum_i \alpha_{B,i}\left(n_i + \frac{1}{2}\right) \quad (45)$$

where B_n is the rotational constant at the nth excited vibrational state along axis B and $\alpha_{B,i}$ is the vibration-rotational coupling constants of the ith normal vibrational mode. The vibration-rotational effect at the ground vibrational state can be easily included by replacing equilibrium rotation constant B_e with the B_0 when calculating the Q_{rot}. As for the vibration-rotational coupling involving excited vibrational states, Richet et al. (1977) suggested using a correction factor to account for the vibrational-rotational coupling involving excited vibrational states. For diatomic molecules, the correction factor is

$$1 + \frac{\delta}{\exp(u) - 1} \quad (46)$$

where $u_i = \frac{h\omega_i}{k_B T}$ and $\delta = \frac{\alpha_e}{B_0}$.

For polyatomic molecules, the correction factor is

$$\prod_i \left[1 + \frac{1}{2}\frac{\delta_i}{\exp(u_i) - 1}\right]^{d_i} \quad (47)$$

where d_i is the degeneracy of the ith vibration mode, and δ_i is a constant that can be calculated by vibration-rotation coupling constants along three principal rotational axis and the rotational constants at ground vibrational state:

$$\delta_i = \frac{\alpha_{i,A}}{A_0} + \frac{\alpha_{i,B}}{B_0} + \frac{\alpha_{i,C}}{C_0} \quad (48)$$

2.7. The correction for BOA

The Born-Oppenheimer approximation (BOA) is one of the most fundamental concepts underlying the framework of quantum chemistry. Under this approximation, the motions of the nuclei and the electrons can be separated and therefore become easier to treat in theory. For a molecule under BOA, its total electronic Hamiltonian can be expressed as

$$\hat{H}_e = -\frac{1}{2}\sum_{i=1}^{N} \nabla_i^2 - \sum_{A=1}^{M}\sum_{i=1}^{N}\frac{Z_A}{r_{Ai}} + \sum_{i=1}^{N}\sum_{j>i}^{N}\frac{1}{r_{ij}} \quad (49)$$

A direct consequence of this approximation is that all isotopologues of a molecule will have identical wavefunctions and electronic energies. In addition, this approximation allows the use of the concept of potential energy surface (PES), and makes it possible to use approximated analytic expression for the PES, e.g., the harmonic approximation ways of the calculation of molecular vibrations, or a quartic or Morse potential for vibrational anharmonicity analysis. However, the electronic energy difference beyond the BOA may affect isotope fractionation behavior under super-cold conditions. If we take the energy correction for the BOA into account, the PES of one molecule and its isotopologues must be slightly different. Whether this difference can be ignored or not? Previous studies pointed that this difference can be safely ignored (e.g., Kleinman and Wolfsberg, 1974b; Valeev and Sherrill, 2003). As a result, this energy correction can be independently imported and there is no need to obtain the molecular constants of different isotopologues under a framework beyond the BOA.

Born and Huang (1956) derived a first-order perturbative result for this correction which called the Diagonal Born-Oppenheimer Correction (DBOC). The DBOC can be calculated through the electronic wavefunction of a molecule by

$$E_{DBOC} = \sum_{i=1}^{M}\left\langle \Psi_e \middle| -\frac{\nabla_{R,i}^2}{2M_i} \middle| \Psi_e \right\rangle = \sum_{i=1}^{M}\int \Psi_e^* \left(-\frac{\nabla_{R,i}^2}{2M_i}\right)\Psi_e d\tau \quad (50)$$

where M_i is the mass of the ith atom of the molecule and $\nabla_{R,i}^2$ means to take the second-order derivative relative to the coordinate of the ith nucleus of the molecule and the integration is calculated relative to the coordinates of the

electron. For an isotopologue pair, the correction factor k_{DBOC} caused by this energy difference can be expressed as

$$k_{DBOC}(AX_H/AX_L) = \exp\left[-\frac{E_{DBOC}(AX_H) - E_{DBOC}(AX_L)}{k_B T}\right] \quad (51)$$

There are many works that have discussed this energy correction (e.g., Kleinman and Wolfsberg, 1973, 1974a, 1974b; Bardo and Wolfsberg, 1975, 1977, 1978; Bardo et al. 1978; Mead and Truhlar, 1979; Handy et al., 1986; Schwartz and Le Roy, 1987; Postma et al., 1988; Ioannou et al., 1996; Goncalves and Mohallem, 2003; Valeev and Sherrill, 2003; Tajti et al., 2004, 2007; Mielke et al., 2005, 2009; Bomble et al., 2006; Gauss et al., 2006; Bubin and Adamowicz, 2007; Jansen et al., 2007; Karton et al., 2007; Harding et al., 2008b; Mohallem, 2008; Pachucki and Komasa, 2008, 2009; Holka et al., 2011; Liévin et al., 2011; Przybytek and Jeziorski, 2012; Pfeiffer et al., 2013; Gidopoulos and Gross, 2014; Tubman et al., 2014; Imafuku et al., 2016; Lutz and Hutson, 2016). However, only a few of these studies focused on the isotope effect of this energy correction (Kleinman and Wolfsberg, 1973, 1974a, 1974b; Bardo and Wolfsberg, 1975, 1976 1977, 1978; Bardo et al., 1978; Postma et al., 1988; Chakraborty et al. 2014; Lutz and Hutson, 2016). Lutz and Hutson (2016) calculated this correction at the CCSD level for many diatomic molecules comprised of alkali- and alkali-earth metals (in addition to Yb_2) and their isotopologues. They discussed the application on the spectroscopy of ultracold molecules (isotopic mass shift) to explore fundamental physical problems. Therefore, a systematic evaluation of the DBOC isotope effect for different molecules is necessary.

2.8. Inversion splitting

In some non-planar molecules (e.g., NH_3), each vibrational or rotational energy level is doubled because of the inversion splitting (McDowell, 1990), which results from the quantum tunneling. It will split the vibrational levels into two sublevels (i.e., symmetric E_s and asymmetric E_{as}) with an energy difference of $\Delta_v = E_{as} - E_s$ about several cm^{-1} and also split the rotational energy levels with an energy difference of Δ_r, corresponding to a minor shift of the rotational constants B_0 (i.e., $\Delta B = B_{0,as} - B_{0,s}$). It is natural to infer that this type of energy level splitting will change the values of Q_{vib} and Q_{rot}. Here we assume that our calculated energy levels are all the lower energy states just like what previous work did (Born and Wolfsberg, 1972). In addition, we just calculated the contribution of this effect at the ground vibrational and rotational state due to the low temperatures.

For vibrational ground state, the correction factor k_{v_inv} caused by the inversion splitting can be expressed by

$$k_{v_inv} \approx \frac{1}{2}\left[1 + \exp\left(\frac{-hc\Delta_{0v}}{k_B T}\right)\right] \quad (52)$$

where Δ_{0v} is the experimentally observed splitting energy difference at ground vibrational state. In this study, this energy difference is 0.7935 and 0.406 cm^{-1} for NH_3 and NH_2D (Weiss and Strandberg, 1951), corresponding to k_{v_inv} values of 0.9943 and 0.9971 at 100 K, respectively.

For rotational levels, the correction factor k_{r_inv} is

$$k_{r\_inv} \approx \frac{1}{2}\left[\frac{Q_{rot}(A_0 + \Delta A, B_0 + \Delta B, C_0 + \Delta C)}{Q_{rot}(A_0, B_0, C_0)} + 1\right] \quad (53)$$

where ΔA, ΔB and ΔC are the observed shifts on the rotational constants. In this study, these shifts are $\Delta A = 0.0020\ cm^{-1}$, $\Delta B = -0.0050\ cm^{-1}$ for NH_3 (Benedict and Plyler, 1956), and $\Delta A = -0.001070\ cm^{-1}$, $\Delta B = -0.000354\ cm^{-1}$ and $\Delta C = -0.000273\ cm^{-1}$ for NH_2D (Snels et al., 2006), corresponding to almost constant k_{r_inv} values of 1.00009 and 1.00006 for NH_3 and NH_2D from 50 to 300 K, respectively. As a result, the correction of the inversion splitting effect for vibrational energy levels must be considered under super-cold conditions, but for rotational energy levels, this splitting effect can be safely ignored (for NH_3 and NH_2D, this effect only causes a correction factor less than 1.0001).

3. METHODS

3.1. Calculation of partition function ratios for an isotopologue pair

Using all the corrections in Section 2, the full partition function ratio (denoted as FPFR hereafter) of an isotopologue can be calculated by

$$FPFR(AX_H/AX_L) = \frac{(Q_{vib}Q_{rot}f_c k_{v\_inv})_{AX_H}}{(Q_{vib}Q_{rot}f_c k_{v\_inv})_{AX_L}} \left(\frac{M_{AX_H}}{M_{AX_L}} \Big/ \frac{m_{X_H}}{m_{X_L}}\right)^{\frac{3}{2}} \times \frac{k_{DBOC}(AX_H/AX_L)}{k_{DBOC}(X_H/X_L)} \quad (54)$$

In addition, every specific contributions from different partition function ratios and correction factors, which are in acronyms defined at below:

TRANS (translational partition function ratio): $\frac{(Q_{trans})_{AX_H}}{(Q_{trans})_{AX_L}} \Big/ \frac{(Q_{trans})_{X_H}}{(Q_{trans})_{X_L}} = \left(\frac{M_{AX_H}}{M_{AX_L}} \Big/ \frac{m_{X_H}}{m_{X_L}}\right)^{\frac{3}{2}}$;

VIB (vibrational partition function ratio including anharmonicity): $\frac{(Q_{vib})_{AX_H}}{(Q_{vib})_{AX_L}}$;

ROT (rotational partition function ratio with nuclear-spin effect): $\frac{(Q_{rot})_{AX_H}}{(Q_{rot})_{AX_L}}$;

CENTDIS (centrifugal distortion correction factor ratio): $\frac{(f_c)_{AX_H}}{(f_c)_{AX_L}}$;

VIBROT (vibration-rotational coupling correction factor ratio): $\frac{(k_{vib\_rot})_{AX_H}}{(k_{vib\_rot})_{AX_L}}$;

INV (inversion splitting correction factor ratio): $\frac{(k_{v_inv})_{AX_H}}{(k_{v_inv})_{AX_L}}$;

DB (DBOC correction factors for FPFR): $\frac{k_{DBOC}(AX_H/AX_L)}{k_{DBOC}(X_H/X_L)}$.

3.2. Quantum chemistry calculation methods

The equilibrium structures and molecular constants of H_2, HF, HCl, H_2O, H_2S, NH_3, HCHO and their isotopologues are calculated using the MP2 method (Møller and Plesset, 1934) with the aug-cc-pVTZ basis set (Dunning, 1989; Woon and Dunning, 1993) by *Gaussian09* software (Frisch et al., 2009) based on the method developed by Barone (2005). The anharmonic frequency analysis of CH_4 is performed by using the *CFOUR* package (CFOUR, 2000; Harding et al., 2008a) at the same theoretical level and basis set because the anharmonic vibration analysis for spherical-top molecules is not supported in *Gaussian09*. Previous works have shown that the MP2 method with large basis sets (e.g., aug-cc-pVTZ) is very useful and reasonably accurate for approximate calculations of low lying vibrational levels (Barone, 2005; Liu et al., 2010). For CH_4, the calculated C-H bond length and harmonic vibrational frequencies are agreed within errors of 0.000001 Å and 0.002 cm^{-1} between these two programs, which had negligible effect on the final calculated FPFR values.

However, the anharmonic treatment of the linear molecules (e.g., HCN and DCN) is still under testing in *Gaussian09*, which means that our results for HCN and DCN may be problematic. Therefore, we also calculated the molecular constants of these molecules using the *CFOUR* packages. Then we calculated the FPFR values using the two sets of data, and they agreed within 0.23% (see Table S6 in Supplementary file). In addition, all the molecules considered here are closed-shell species, and we did not consider open-shell species such as O_2, NO and NO_2 since the anharmonic vibration analysis results at MP2 level with a relatively large basis set (e.g., aug-cc-pVTZ) may be problematic due to the spin contamination, requiring a DFT method that was recommended for such systems by Barone (2005).

As for the DBOC, we adopt the methods built in the *CFOUR* package (Harding et al., 2008a) to calculate this energy correction. Gauss et al. (2006) developed the methods of using configuration-interaction and coupled-cluster theory to accurately evaluate the DBOC and implemented them into the Mainz-Austin-Budapest Version of the *ACESII* package, which later became known as the *CFOUR*. Their method made it possible to accurately calculate this energy correction with a comparable cost as a harmonic frequency analysis at the same theoretical level. The *CFOUR* program can calculate the DBOC at HF-SCF, MP2 and CCSD levels. Tajti et al. (2007) and Tajti et al. (2007) compared the results of different methods and basis sets. Gauss et al. (2006) recommended the CCSD/aug-cc-pCVTZ level for the DBOC calculation with a suggested converged value to about 1–2 cm^{-1}. Also, Tajti et al. (2007) evaluated the differences between the coupled cluster and the perturbation theory methods on the calculation of DBOC. Their results showed that DBOC under the MP2 scheme could be comparable for most cases (except some special molecules such as NO) to the much more computationally expensive CCSD treatments. In this study, when the system is large, the DBOC calculation is performed at MP2/cc-pVTZ level, and for small molecules, a much more computationally expensive calculation at CCSD/aug-cc-pCVTZ level is adopted.

4. RESULTS

4.1. Frequencies and molecular constants

The calculated fundamental frequencies are compared with the experimental results of H_2, HF, HCl, HCN, H_2O, H_2S, NH_3, HCHO, CH_4 and their isotopologues in Table 1. Generally, our calculated frequencies are in good agreement with the experimental ones. However, for H-bearing diatomic molecules, e.g., H_2 and HCl, the MP2 method obviously overestimated the fundamental frequencies. This overestimation is probably a result of inadequacy of the theoretical method we used. Fig. 2 shows that the calculated and experimental fundamentals fall into a line with

Table 1
Calculated and experimentally measured fundamental vibrational frequencies.

Frequency (cm^{-1})			Frequency (cm^{-1})			Frequency (cm^{-1})		
Molecule	Exp.	Calc.	Molecule	Exp.	Calc.	Molecule	Exp.	Calc.
H_2	4161	4283	HDO	3707	3732	DCHO	2844	2900
HD	3632	3737		2727	2742		2121	2125
HF	3962	3964		1402	1387		1723	1713
DF	2907	2908	H_2S	2626	2701		1400	1409
HCl	2886	2959		2615	2688		1074	1078
DCl	2091	2142		1183	1198		1041	1031
HCN	3312	3357	NH_3	3444	3502	CH_4	3019	3074
	2089	2013		3337	3392		2917	2970
	712	731		1627	1626		1534	1558
DCN	2630	2630		950	945		1306	1324
	1925	1875	HCHO	2843	2866	CH_3D	3017	3071
	569	577		2782	2849		2945	2996
H_2O	3756	3785		1746	1735		2200	2234
	3657	3677		1500	1516		1471	1494
	1595	1577		1249	1251		1300	1320
				1167	1190		1155	1174

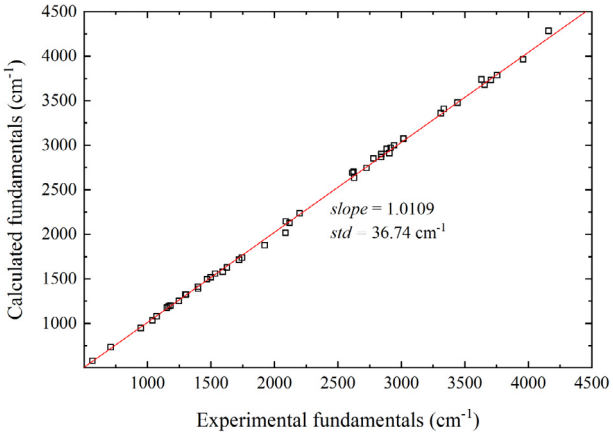

Fig. 2. Comparison of the calculated and experimental fundamentals.

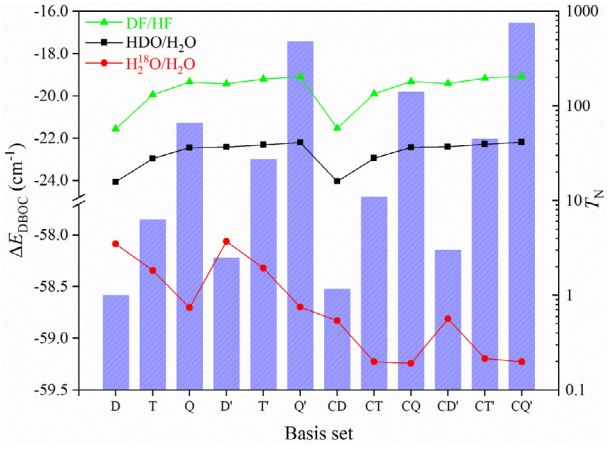

Fig. 3. Calculated DBOC differences of DF/HF, HDO/H_2O and $H_2^{18}O/H_2O$ isotopologues at CCSD level with different basis sets and relative calculation times (H_2O) compared with CCSD/cc-pVDZ result. The symbols in the horizontal axis denote different basis sets (X = cc-pVnZ; X' = aug-cc-pVnZ; CX = cc-pCVnZ; CX' = aug-cc-pCVnZ; n = D, T, Q). The left Y-axis denotes the calculated DBOC difference of an isotopologue pair (expressed as broken lines). The right Y-axis shows the calculation time of the DBOC value of the H_2O using different basis set (expressed as blue bars and all the calculation time has been normalized to the time consumed at CCSD/cc-pVDZ level). (For interpretation of the references to color in this figure legend, the reader is referred to the web version of this article.)

a slope of 1.0109, with an R-square value as 0.9998. The fitting result means that our calculation overestimated the fundamental frequencies about 1.09% in average. However, the deviations are mainly from those high frequencies which are not sensitive to isotope exchange. Therefore, we have not applied the scaling treatment in this study. All the molecular constants are listed in Tables S1–S5 of Supplementary File.

4.2. DBOC corrections

Using the *CFOUR* program, the DBOC values are calculated for all the molecules we studied. To guarantee the accuracy of our calculation, we firstly use H_2O, HF and their isotopologues to test the influences of different theoretical levels and different equilibrium structures on the calculated DBOC values.

We have tested different basis sets, including cc-pVnZ (Dunning, 1989; Woon and Dunning, 1993), aug-cc-pVnZ (Dunning, 1989; Woon and Dunning, 1993), cc-pCVnZ (Dunning, 1989; Woon and Dunning, 1995; Peterson and Dunning, 2002) and aug-cc-pCVnZ (Dunning, 1989; Woon and Dunning, 1995; Peterson and Dunning, 2002), where n = D, T and Q, to check the convergence of the DBOC for an isotopologue pair (HDO/H_2O or $H_2^{18}O/H_2O$). The basis sets which include the core electron correlation effect (cc-pCVnZ and aug-cc-pCVnZ where n = D, T and Q) have no definitions for H and He. The testing results are shown in Fig. 3. The left Y-axis denotes the DBOC difference of an isotopologue pair calculated by $E_{DBOC}(AX_H) - E_{DBOC}(AX_L)$ which presented by green (DF/HF), black (HDO/H_2O) and red ($H_2^{18}O/H_2O$) broken lines. The right side of the Y-axis shows the computational time consumed (Normalized to the CCSD/cc-pVDZ level) when calculating the E_{DBOC} of H_2O with different basis sets, which expressed as blue bars. The X-axis denotes the basis sets used by simple abbreviations (X = cc-pVnZ; X' = aug-cc-pVnZ; CX = cc-pCVnZ; CX' = aug-cc-pCVnZ; n = D, T and Q). Generally, we can see that the ΔE_{DBOC} variations are about 2 cm^{-1} for the pair of DF/HF and HDO/H_2O, and 1.5 cm^{-1} for the pair of $H_2^{18}O/H_2O$ for all the basis sets being tested. Then, for H/D systems we considered here (DF/HF and HDO/H_2O pair), the inclusion of the diffuse function has significant effect on the results. For example, ΔE_{DBOC} (DF/HF) changes from -21.555 cm^{-1} to -19.425 cm^{-1} when the basis set changes from cc-pVDZ to aug-cc-pVDZ. However, for $H_2^{18}O/H_2O$ pair, the effect of the diffuse function is relatively small and can be negligible (i.e., from -58.086 cm^{-1} to -58.064 cm^{-1} when basis set changes from cc-pVDZ to aug-cc-pVDZ). In addition, the effect of the core-electron correlation can also significantly change the result for $H_2^{18}O/H_2O$ pair, from -58.086 cm^{-1} to -58.829 cm^{-1} when the basis set changes from cc-pVDZ to cc-pCVDZ. For DF/HF and HDO/H_2O, the effect of the core-electron correlation is small (DF/HF: -21.555 cm^{-1} to -21.529 cm^{-1}; HDO/H_2O: -24.065 cm^{-1} to -24.045 cm^{-1}, basis set changes from cc-pVDZ to cc-pCVDZ). Finally, when the effects of the diffuse function and the core-electron correlation are both taken into account, we can see that the results converged within 0.1 cm^{-1} when basis set changes from aug-cc-pCVTZ to aug-cc-pCVQZ. In the end, we adopt the aug-cc-pCVTZ as the basis set for our calculation for the H/D systems due to its accuracy and efficiency (only 10% of the time consumed by aug-cc-pCVQZ). In addition, we just need to perform a DBOC calculation only once for each molecule. The DBOC values of its other isotopologues can be easily obtained by running the *CFOUR* packages immediately after a full DBOC calculation was finished.

The DBOC involves calculation of the second-derivatives relative to the nuclear coordinates, so it must be structure-dependent. Therefore, the structure sensitivity

of the DBOC calculations on 8 kinds of different structures of H_2O are checked at the CCSD/aug-cc-pCVTZ level (7 structures optimized with different quantum chemistry methods + 1 experimentally determined structure. Detailed information about these structures is listed in Table S7 in Supplementary file). The results listed in Table 2 indicate that minor equilibrium structure differences have negligible effects on the final values of DBOC (generally $< 0.05\ cm^{-1}$).

Table 3a shows all the DBOC values calculated in this study for H_2, HF, HCl, H_2O, H_2S, NH_3, CH_4, HCHO and their D-substituted isotopologues based on the MP2/aug-cc-pVTZ optimized geometries. For partition function ratios of an isotopologue pair, the correction caused by DBOC is $\frac{k_{DBOC}(AD/AH)}{k_{DBOC}(D/H)}$ (see Eq. (54)), which ranges from $-4.134\ cm^{-1}$ (DCHO/HCHO – D/H) to $10.716\ cm^{-1}$ (DF/HF – D/H), corresponding to a correction factor from 1.0200 to 0.9499 at 300 K. And we also compared our results in Table 3b with previous DBOC calculations (Kleinman and Wolfsberg, 1973, 1974a; Bardo and Wolfsberg, 1978; Bardo et al., 1978). These results showed the necessity of adding the electron-correlation contributions (both valence and core electrons) to the DBOC values. Previous calculations did not include the electron-correlation effect except for Bardo et al. (1978), which estimated it by using a configuration interaction method.

From our results, the DBOC has significant effects on the final calculation of H/D isotope fractionations for systems at both low and high temperatures. For example, we have found that this correction can change the FPFR values of organic molecules by several percent even at 300 K. It may cause serious problems when one calculates H/D fractionations of organic molecules without considering this effect. Unfortunately, to the best of our knowledge, there is no theoretical work that considers this correction right now in stable isotope geochemistry field. To have some preliminary ideas of how large this effect will be for organic molecules, we have calculated several important organic molecules at CCSD/aug-cc-pCVTZ level (for small organic molecules) and MP2/cc-pVTZ (for large organic molecules) (Table 4). Our MP2 calculation reproduced most DBOC values relative to the CCSD ones (99.5% in average) which just like the conclusion of Tajti et al. (2007), and corresponding correction factors are in agreement within 0.3%.

Table 3a
Calculated DBOC values at the CCSD/aug-cc-pCVTZ level.

Molecule	DBOC (cm^{-1})	Molecule	DBOC (cm^{-1})
H	59.682	NH_3	598.220
D	29.856	NH_2D	572.984
H_2	114.652	CH_4	595.116
HD	86.003	CH_3D	566.401
HF	624.151		
DF	605.041	Isotopologue pair	DBOC (cm^{-1})
HCl	1385.903	D/H	−29.826
DCl	1361.521	HD/H_2	−28.649
HCN	872.191	DF/HF	−19.110
DCN	846.240	DCl/HCl	−24.382
H_2O	620.588	DCN/HCN	−25.950
HDO	598.323	HDO/H_2O	−22.265
H_2S	1384.903	HDS/H_2S	−27.546
HDS	1357.357	NH_2D/NH_3	−25.236
HCHO	1036.116	CH_3D/CH_4	−28.715
DCHO	1002.157		

4.3. FPFR values at super-cold conditions

Using the equations listed in Section 3.1, the natural logarithms of FPFR values and contributions from different partition function ratios and corrections of HD/H_2, DF/HF, DCl/HCl, DCN/HCN, HDO/H_2O, HDS/H_2S, DCHO/HCHO, NH_2D/NH_3 and CH_3D/CH_4 from 50 to 200 K are calculated and listed in Tables 5.1–5.9 and summarized in Table 6. The results of "RPFR" are those directly using the B-M equation with the harmonic frequencies along with a zero-point energy scaling treatment (scaling factor S_{ZPE} is as 0.985).

For a FPFR value, the contribution of each items proposed in Section 3.1 varies differently except for the TRANS item which is a temperature-independent constant. Generally, the VIB contribution dominates a FPFR value. The contribution of the rotational motion (ROT) is quite different from that of the Urey model. In the Urey model, the ROT is temperature-independent and always bigger than unity as a result of the Teller-Redlich theorem (Redlich, 1935; Wilson et al., 1955). In contrast, the ROT value changes significantly as the temperature decreases due to the quantum mechanical treatment of rotation with the consideration of nuclear-spin weights. Also, the DBOC

Table 2
Calculated DBOC with CCSD/aug-cc-pCVTZ method using different optimized geometries.

Geometry[a]	HDO/H_2O	$H_2^{18}O/H_2^{16}O$	HD/H_2
B3LYP/6-31G(d, p)	−22.242	−59.197	−28.571
MP2(fc)/aug-cc-pVTZ	−22.317	−59.199	−28.649
MP2/aug-cc-pVTZ	−22.340	−59.198	−28.648
MP4(fc)/aug-cc-pVTZ	−22.254	−59.196	−28.588
MP4/aug-cc-pVTZ	−22.273	−59.196	−28.588
CCSD(T, fc)/aug-cc-pVQZ	−22.277	−59.196	−28.583
CCSD(T) /aug-cc-pVQZ	−22.286	−59.196	−28.583
Expt.	−22.283	−59.196	−28.591

fc: Frozen-core calculation.
[a] All geometries data are from Computational Chemistry Comparison and Benchmark DataBase (CCCBDB).

Table 3b
DBOC values (this study vs. previous works).

Molecule and reactions	DBOC (cm^{-1}) This study	DBOC (cm^{-1}) Other works
H	59.682	59.77[a]
D	29.856	29.90[a]
H_2	114.652	114.59[a]
HD	86.003	
HCl	1385.903	1361.59[a]
DCl	1361.521	1331.78[a]
$HF + HD = DF + H_2$	9.538	7.77[b]
	9.538	7.599[c]
$HCl + HD = DCl + H_2$	4.267	3.25[b]
$H_2O + HD = HDO + H_2$	6.383	3.75[d]
$H_2O + D_2 = D_2O + H_2$	12.767	7.51[d]
$H_2 + D = HD + H$	1.177	4.55[d]

[a] Bardo et al. (1978): Configuration interaction results.
[b] Kleinman and Wolfsberg (1974a): LCAO-MO-SCF results.
[c] Kleinman and Wolfsberg (1973): LCAO-MO-SCF results.
[d] Bardo and Wolfsberg (1978): LCAO-MO-SCF results.

Table 4
Calculated DBOC values for some organic molecules at the CCSD/aug-cc-pCVTZ and MP2/cc-pVTZ level and corresponding correction factor k for the FPFR values at 300 K.

Isotopologue pair	$DBOC_{MP2}$ (cm^{-1})	k_{MP2}	$DBOC_{CCSD}$ (cm^{-1})	k_{CCSD}
D/H	−29.855	–	−29.826	–
CH_3D/CH_4	−28.514	0.9936	−28.704	0.9946
C_2H_5D/C_2H_6	−29.254	0.9971	−29.414	0.9980
C_2H_3D/C_2H_4	−29.047	0.9961	−29.422	0.9981
HC≡CD/HC≡CH	−25.938	0.9814	−26.469	0.9840
DCHO/HCHO	−33.683	1.0185	−33.837	1.0194
CH_3OD/CH_3OH	−23.250	0.9688	−23.081	0.9682
CH_2DOH/CH_3OH	−30.119	1.0013	−30.119	1.0013
HCOOD/HCOOH	−20.803	0.9575	−20.958	0.9584
DCOOH/HCOOH	−29.843	0.9999	−29.874	1.0002
$CH_3C≡CD/CH_3C≡CH$	−26.181	0.9825	–	
$CH_2DC≡CH/CH_3C≡CH$	−28.051	0.9914	–	
CH_3CDO/CH_3CHO	−36.885	1.0343	–	
CH_2DCHO/CH_3CHO	−28.650	0.9942	–	
C_6H_5D/C_6H_6	−28.993	0.9959	–	

Table 5.1
Calculated logarithms of FPFR with our method and the Urey model (RPFR), and VIB, ROT, CENTDIS, VIBROT and DB values of HD/H_2 at 50–200 K.

T(K)	VIB	ROT	CENTDIS	VIBROT	DB	FPFR	RPFR
50	8.5538	0.6537	0.0001	−0.0080	−0.0339	8.7347	8.4203
60	7.1282	0.5954	0.0001	−0.0109	−0.0282	7.2534	6.9930
70	6.1099	0.5338	0.0001	−0.0121	−0.0242	6.1763	5.9735
80	5.3461	0.4776	0.0001	−0.0122	−0.0212	5.3593	5.2088
90	4.7521	0.4298	0.0001	−0.0116	−0.0188	4.7205	4.6141
100	4.2769	0.3908	0.0001	−0.0107	−0.0169	4.2091	4.1383
110	3.8881	0.3596	0.0001	−0.0097	−0.0154	3.7916	3.7491
120	3.5641	0.3351	0.0001	−0.0087	−0.0141	3.4454	3.4247
130	3.2899	0.3160	0.0001	−0.0077	−0.0130	3.1541	3.1502
140	3.0549	0.3013	0.0001	−0.0069	−0.0121	2.9062	2.9149
150	2.8513	0.2900	0.0001	−0.0061	−0.0113	2.6929	2.7110
160	2.6731	0.2815	0.0001	−0.0055	−0.0106	2.5075	2.5326
170	2.5158	0.2752	0.0001	−0.0049	−0.0100	2.3451	2.3752
180	2.3761	0.2705	0.0001	−0.0044	−0.0094	2.2017	2.2353
190	2.2510	0.2672	0.0001	−0.0041	−0.0089	2.0742	2.1101
200	2.1385	0.2648	0.0001	−0.0037	−0.0085	1.9600	1.9974

Table 5.2
Calculated logarithms of FPFR with our method and the Urey model (RPFR), and VIB, ROT, CENTDIS, VIBROT and DB values of DF/HF at 50–200 K.

T(K)	VIB	ROT	CENTDIS	VIBROT	DB	FPFR	RPFR
50	16.1294	0.5450	0.0000	−0.0027	−0.3084	15.3984	15.8026
60	13.4412	0.5620	0.0000	−0.0031	−0.2570	12.7781	13.1153
70	11.5210	0.5740	0.0000	−0.0034	−0.2203	10.9063	11.1957
80	10.0809	0.5829	0.0000	−0.0037	−0.1927	9.5024	9.7560
90	8.9608	0.5897	0.0000	−0.0038	−0.1713	8.4104	8.6363
100	8.0647	0.5952	0.0000	−0.0040	−0.1542	7.5368	7.7405
110	7.3315	0.5996	0.0000	−0.0041	−0.1402	6.8220	7.0076
120	6.7206	0.6033	0.0000	−0.0042	−0.1285	6.2263	6.3968
130	6.2036	0.6064	0.0000	−0.0043	−0.1186	5.7223	5.8800
140	5.7605	0.6091	0.0000	−0.0043	−0.1101	5.2902	5.4370
150	5.3765	0.6114	0.0000	−0.0044	−0.1028	4.9158	5.0531
160	5.0404	0.6134	0.0000	−0.0044	−0.0964	4.5881	4.7172
170	4.7439	0.6152	0.0000	−0.0045	−0.0907	4.2990	4.4208
180	4.4804	0.6168	0.0000	−0.0045	−0.0857	4.0421	4.1573
190	4.2446	0.6182	0.0000	−0.0045	−0.0811	3.8121	3.9216
200	4.0323	0.6194	0.0000	−0.0046	−0.0771	3.6052	3.7094

Table 5.3
Calculated logarithms of FPFR with our method and the Urey model (RPFR), and VIB, ROT, CENTDIS, VIBROT and DB values of DCl/HCl at 50–200 K.

T(K)	VIB	ROT	CENTDIS	VIBROT	DB	FPFR	RPFR
50	12.2948	0.6143	0.0000	−0.0030	−0.1567	11.7523	11.9220
60	10.2457	0.6229	0.0000	−0.0032	−0.1305	9.7377	9.8796
70	8.7820	0.6289	0.0000	−0.0033	−0.1119	8.2986	8.4208
80	7.6843	0.6335	0.0000	−0.0034	−0.0979	7.2193	7.3266
90	6.8305	0.6370	0.0000	−0.0034	−0.0870	6.3798	6.4756
100	6.1474	0.6398	0.0000	−0.0035	−0.0783	5.7082	5.7948
110	5.5886	0.6421	0.0000	−0.0035	−0.0712	5.1587	5.2378
120	5.1229	0.6440	0.0000	−0.0036	−0.0653	4.7008	4.7736
130	4.7288	0.6456	0.0000	−0.0036	−0.0603	4.3134	4.3808
140	4.3910	0.6470	0.0000	−0.0036	−0.0559	3.9812	4.0442
150	4.0983	0.6482	0.0000	−0.0036	−0.0522	3.6934	3.7524
160	3.8421	0.6492	0.0000	−0.0037	−0.0490	3.4416	3.4971
170	3.6161	0.6501	0.0000	−0.0037	−0.0461	3.2193	3.2718
180	3.4152	0.6509	0.0000	−0.0037	−0.0435	3.0218	3.0716
190	3.2355	0.6517	0.0000	−0.0037	−0.0412	2.8451	2.8924
200	3.0737	0.6523	0.0000	−0.0037	−0.0392	2.6860	2.7312

correction (DB) can also significantly change the FPFR value under super-cold conditions (e.g., The DB value for HD/H_2 pair can change from 0.9667 to 0.9916 at the temperature range of 50–200 K). The biggest difference we found for simple gaseous H/D system is the DF/HF pair ($10.716\ cm^{-1}$ relative to D/H pair) which means the DB value is 0.9499 even at 300 K. The DF/HF pair may not be geochemically significant, but we think it is necessary to emphasis the importance of the DBOC in isotope fractionation calculation.

4.4. Equilibrium constants of isotopic exchange reactions

Table 7 shows the calculated equilibrium constants of some isotopic exchange reactions at ambient temperatures and the comparisons with previous theoretical and experimental results. For an isotopologue pair, the DBOC difference can be written as (from Eq. (50))

$$E_{DBOC}(AX_H/AX_L) = E_{DBOC}(AX_H) - E_{DBOC}(AX_L) = \left\langle \Psi_e \middle| -\frac{\frac{2}{R,X}}{2}\left(\frac{1}{m_{X_H}} - \frac{1}{m_{X_L}}\right) \middle| \Psi_e \right\rangle = \frac{m_{X_H} - m_{X_L}}{2m_{X_H}m_{X_L}} \langle \Psi_e |^2_{R,X} | \Psi_e \rangle \quad (55)$$

Note that E_{DBOC} will be zero for a reaction like $H_2 + D_2 = 2HD$, due to exactly identical electronic wavefunction Ψ_e for all the three isotopologues (Bardo and Wolfsberg, 1975). Therefore, we don't have to evaluate the contribution of DBOC when dealing with this kind of isotopic exchange reactions.

The calculated results in Table 7 are in excellent agreement with experimental works at ambient temperatures. There is no equilibrium isotope fractionation experiment at super-cold conditions (<200 K) at present for the comparison. The data provided in Table 7 appear to be the first

Table 5.4
Calculated logarithms of FPFR with our method and the Urey model (RPFR), and VIB, ROT, CENTDIS, VIBROT and DB values of DCN/HCN at 50–200 K.

T(K)	VIB	ROT	CENTDIS	VIBROT	DB	FPFR	RPFR
50	17.3336	0.1980	0.0000	−0.0011	−0.1115	16.4353	16.4626
60	14.4446	0.1984	0.0000	−0.0011	−0.0929	13.5654	13.5883
70	12.3811	0.1988	0.0000	−0.0011	−0.0797	11.5155	11.5353
80	10.8335	0.1990	0.0000	−0.0011	−0.0697	9.9780	9.9955
90	9.6299	0.1992	0.0000	−0.0011	−0.0620	8.7824	8.7981
100	8.6672	0.1993	0.0000	−0.0011	−0.0558	7.8260	7.8404
110	7.8798	0.1994	0.0000	−0.0011	−0.0507	7.0438	7.0571
120	7.2240	0.1995	0.0000	−0.0011	−0.0465	6.3923	6.4048
130	6.6695	0.1996	0.0000	−0.0011	−0.0429	5.8414	5.8534
140	6.1948	0.1997	0.0000	−0.0011	−0.0398	5.3698	5.3814
150	5.7840	0.1997	0.0000	−0.0011	−0.0372	4.9617	4.9730
160	5.4252	0.1998	0.0000	−0.0011	−0.0349	4.6053	4.6163
170	5.1092	0.1998	0.0000	−0.0011	−0.0328	4.2914	4.3023
180	4.8291	0.1999	0.0000	−0.0012	−0.0310	4.0131	4.0240
190	4.5791	0.1999	0.0000	−0.0012	−0.0293	3.7648	3.7756
200	4.3547	0.1999	0.0000	−0.0012	−0.0279	3.5419	3.5528

Table 5.5
Calculated logarithms of FPFR with our method and the Urey model (RPFR), and VIB, ROT, CENTDIS, VIBROT and DB values of HDO/H_2O at 50–200 K.

T(K)	VIB	ROT	CENTDIS	VIBROT	DB	FPFR	RPFR
50	17.7630	0.4764	0.0002	−0.0031	−0.2176	17.0619	17.5165
60	14.8025	0.4815	0.0002	−0.0032	−0.1813	14.1427	14.5219
70	12.6879	0.4852	0.0002	−0.0033	−0.1554	12.0575	12.3830
80	11.1019	0.4879	0.0003	−0.0034	−0.1360	10.4937	10.7788
90	9.8684	0.4900	0.0003	−0.0034	−0.1209	9.2773	9.5311
100	8.8815	0.4916	0.0003	−0.0035	−0.1088	8.3042	8.5329
110	8.0741	0.4930	0.0004	−0.0035	−0.0989	7.5080	7.7162
120	7.4013	0.4941	0.0004	−0.0035	−0.0907	6.8446	7.0356
130	6.8319	0.4951	0.0004	−0.0036	−0.0837	6.2832	6.4597
140	6.3439	0.4959	0.0005	−0.0036	−0.0777	5.8020	5.9661
150	5.9210	0.4966	0.0005	−0.0036	−0.0725	5.3849	5.5383
160	5.5510	0.4972	0.0005	−0.0036	−0.0680	5.0200	5.1640
170	5.2244	0.4978	0.0005	−0.0037	−0.0640	4.6981	4.8337
180	4.9342	0.4982	0.0006	−0.0037	−0.0604	4.4119	4.5402
190	4.6745	0.4987	0.0006	−0.0037	−0.0573	4.1558	4.2775
200	4.4408	0.4990	0.0006	−0.0037	−0.0544	3.9254	4.0411

predictions of equilibrium isotope exchange constants under super-cold conditions.

5. DISCUSSION

5.1. Comparisons with low-temperature experiments

To evaluate the accuracy of our method, the equilibrium constants (K_{eq}) of the $NH_3 + HD = NH_2D + H_2$ exchange reaction were calculated and compared with the experimentally determined values at 200–300 K (Herrick and Sabi, 1943; Bigeleisen and Perlman, 1951; Perlman et al., 1953; Ravoire et al., 1963). All the calculations used the same set of data for NH_3, NH_2D, H_2 and HD (see Tables S1 and S4 in the Supplementary file). Comparison results are listed in Fig. 4. The K_{eq} calculated using our method and the B-M equation are expressed as black and red solid lines in Fig. 4. And the K_{eq} is also calculated using the method of Richet et al. (1977) for HD/H_2 and Liu et al. (2010) for NH_2D/NH_3 (the green line). In addition, we also calculated the K_{eq} using our method but without the DBOC correction, which is expressed as a blue line. All the calculations slightly overestimated the K_{eq} to about 3% in average. This is maybe due to the overestimation (~1.1% in average) of the fundamental frequencies in our quantum chemistry calculation (see Section 4.1 and Fig. 3), which will result in a bigger zero-point-vibrational-energy difference and then a bigger K_{eq}. In the four calculated lines, our method (including the DBOC) gives the best prediction when compared with the experimental results. The results of other methods (B-M equation, Richet et al., 1977; Liu et al., 2010) and our method without the DBOC correction are almost the same,

Table 5.6
Calculated logarithms of FPFR with our method and the Urey model (RPFR), and VIB, ROT, CENTDIS, VIBROT and DB values of HDS/H_2S at 50–200 K.

T(K)	VIB	ROT	CENTDIS	VIBROT	DB	FPFR	RPFR
50	13.3482	0.5093	0.0002	−0.0032	−0.0656	12.7941	12.9460
60	11.1235	0.5119	0.0002	−0.0032	−0.0547	10.5829	10.7100
70	9.5344	0.5138	0.0003	−0.0033	−0.0469	9.0035	9.1128
80	8.3426	0.5151	0.0003	−0.0033	−0.0410	7.8190	7.9150
90	7.4157	0.5162	0.0003	−0.0033	−0.0365	6.8976	6.9833
100	6.6741	0.5171	0.0004	−0.0034	−0.0328	6.1606	6.2380
110	6.0674	0.5178	0.0004	−0.0034	−0.0298	5.5575	5.6281
120	5.5618	0.5183	0.0004	−0.0034	−0.0273	5.0550	5.1200
130	5.1339	0.5188	0.0005	−0.0034	−0.0252	4.6298	4.6900
140	4.7672	0.5193	0.0005	−0.0034	−0.0234	4.2654	4.3214
150	4.4494	0.5196	0.0006	−0.0034	−0.0219	3.9495	4.0020
160	4.1714	0.5199	0.0006	−0.0034	−0.0205	3.6732	3.7225
170	3.9261	0.5202	0.0006	−0.0034	−0.0193	3.4293	3.4759
180	3.7080	0.5205	0.0007	−0.0034	−0.0182	3.2126	3.2568
190	3.5129	0.5207	0.0007	−0.0035	−0.0173	3.0188	3.0607
200	3.3374	0.5209	0.0007	−0.0035	−0.0164	2.8444	2.8843

Table 5.7
Calculated logarithms of FPFR with our method and the Urey model (RPFR), and VIB, ROT, CENTDIS, VIBROT and DB values of DCHO/HCHO at 50–200 K.

T(K)	VIB	ROT	CENTDIS	VIBROT	DB	FPFR	RPFR
50	17.8191	0.2993	0.0000	−0.0010	0.1189	17.2473	17.3037
60	14.8492	0.2996	0.0000	−0.0010	0.0991	14.2579	14.3049
70	12.7279	0.2997	0.0000	−0.0010	0.0850	12.1226	12.1629
80	11.1369	0.2999	0.0001	−0.0010	0.0743	10.5211	10.5564
90	9.8995	0.3000	0.0001	−0.0010	0.0661	9.2755	9.3069
100	8.9095	0.3001	0.0001	−0.0010	0.0595	8.2791	8.3073
110	8.0996	0.3001	0.0001	−0.0010	0.0541	7.4638	7.4895
120	7.4246	0.3002	0.0001	−0.0010	0.0496	6.7844	6.8080
130	6.8535	0.3002	0.0001	−0.0010	0.0457	6.2095	6.2313
140	6.3640	0.3003	0.0001	−0.0010	0.0425	5.7168	5.7370
150	5.9398	0.3003	0.0001	−0.0010	0.0396	5.2897	5.3086
160	5.5686	0.3003	0.0001	−0.0010	0.0372	4.9161	4.9338
170	5.2411	0.3003	0.0001	−0.0010	0.0350	4.5865	4.6032
180	4.9501	0.3004	0.0001	−0.0010	0.0330	4.2935	4.3093
190	4.6897	0.3004	0.0001	−0.0010	0.0313	4.0315	4.0464
200	4.4555	0.3004	0.0001	−0.0010	0.0297	3.7957	3.8099

and they both overestimate the K_{eq} when compared with the best prediction (the black line), especially in the low temperature end. Because the calculation difference between the black and blue line is just whether the DBOC is included or not, this offset is directly resulted from the DBOC effect.

If the vibrational fundamentals of these molecules are calculated using much better method (e.g., CCSD method), the black, blue and green lines will be lower and more close to the experimental values (Fig. 4). Whether the DBOC is taking into account or not in the calculations do affect the final result, especially at the low temperature end (200 K). In this way, we can say that the DBOC do affect the isotope fractionation behavior when temperature is low. In addition, the same evaluation has been done for the $D_2 + 2HCl = H_2 + 2DCl$ reaction at 20 °C by Postma et al. (1988). However, more experimental data at supercold temperatures (<200 K) are still needed.

5.2. Comparison with other methods

The study of Liu et al. (2010) illustrated that higher-order corrections to the B-M equation such as vibrational anharmonicity (including G_0 term), quantum mechanical rotation, vibration-rotational coupling and hindered internal rotation (for molecules have internal rotator such as ethane) are necessary for the H/D system in order to compute accurate isotope fractionation factors. However, it is unclear whether the approach of Liu et al. (2010) can produce sufficiently accurate fractionation factors under

Table 5.8
Calculated logarithms of FPFR with our method and the Urey model (RPFR), and VIB, ROT, CENTDIS, VIBROT and DB values of NH_2D/NH_3 at 50–200 K.

T(K)	VIB	ROT	CENTDIS	VIBROT	INV	DB	FPFR	RPFR
50	18.8834	0.3601	0.0002	−0.0066	0.0055	−0.1321	18.1582	18.4143
60	15.7362	0.3639	0.0003	−0.0067	0.0046	−0.1101	15.0357	15.2492
70	13.4881	0.3660	0.0003	−0.0068	0.0039	−0.0943	12.8048	12.9885
80	11.8021	0.3674	0.0004	−0.0068	0.0034	−0.0825	11.1315	11.2929
90	10.4908	0.3684	0.0004	−0.0068	0.0030	−0.0734	9.8300	9.9741
100	9.4417	0.3692	0.0004	−0.0069	0.0027	−0.0660	8.7888	8.9191
110	8.5834	0.3699	0.0005	−0.0069	0.0025	−0.0600	7.9369	8.0559
120	7.8681	0.3704	0.0005	−0.0069	0.0023	−0.0550	7.2270	7.3365
130	7.2629	0.3709	0.0006	−0.0069	0.0021	−0.0508	6.6263	6.7279
140	6.7441	0.3712	0.0006	−0.0069	0.0019	−0.0472	6.1114	6.2062
150	6.2946	0.3716	0.0007	−0.0069	0.0018	−0.0440	5.6653	5.7541
160	5.9012	0.3719	0.0007	−0.0069	0.0017	−0.0413	5.2749	5.3585
170	5.5542	0.3721	0.0007	−0.0069	0.0016	−0.0388	4.9305	5.0095
180	5.2458	0.3724	0.0008	−0.0069	0.0015	−0.0367	4.6244	4.6993
190	4.9698	0.3726	0.0008	−0.0069	0.0014	−0.0348	4.3505	4.4217
200	4.7216	0.3728	0.0009	−0.0069	0.0014	−0.0330	4.1042	4.1720

Table 5.9
Calculated logarithms of FPFR with our method and the Urey model (RPFR), and VIB, ROT, CENTDIS, VIBROT, INV and DB values of CH_3D/CH_4 at 50–200 K.

T(K)	VIB	ROT	CENTDIS	VIBROT	DB	FPFR	RPFR
50	18.1887	0.2928	0.0005	−0.0017	−0.0320	17.5010	17.7850
60	15.1572	0.2952	0.0005	−0.0018	−0.0267	14.4772	14.7132
70	12.9919	0.2964	0.0006	−0.0019	−0.0228	12.3169	12.5191
80	11.3679	0.2971	0.0007	−0.0019	−0.0200	10.6966	10.8736
90	10.1048	0.2976	0.0008	−0.0019	−0.0178	9.4363	9.5937
100	9.0943	0.2980	0.0009	−0.0019	−0.0160	8.4281	8.5698
110	8.2676	0.2984	0.0010	−0.0019	−0.0145	7.6033	7.7320
120	7.5786	0.2987	0.0011	−0.0019	−0.0133	6.9159	7.0339
130	6.9956	0.2989	0.0012	−0.0019	−0.0123	6.3343	6.4432
140	6.4960	0.2991	0.0013	−0.0019	−0.0114	5.8358	5.9369
150	6.0629	0.2993	0.0014	−0.0019	−0.0107	5.4038	5.4980
160	5.6840	0.2995	0.0015	−0.0019	−0.0100	5.0258	5.1141
170	5.3497	0.2996	0.0016	−0.0019	−0.0094	4.6923	4.7753
180	5.0525	0.2997	0.0017	−0.0019	−0.0089	4.3958	4.4742
190	4.7867	0.2998	0.0018	−0.0019	−0.0084	4.1307	4.2048
200	4.5475	0.2999	0.0019	−0.0019	−0.0080	3.8921	3.9624

super-cold conditions, so a comparison is needed at super-cold conditions.

We calculated the relative differences of our method with the B-M equation and the method proposed by Liu et al. (2010) from 50 to 300 K using the same set of molecular constants listed in the Supplementary file. The relative difference between the B-M equation and our method is denoted as (RPFR/FPFR − 1) * 100, the RPFR values are calculated using Eq. (9) with a 0.985 ZPE scaling factor. All the isotopologue pairs considered in this study were compared and the results are illustrated in Fig. 5(a). We can see that the B-M equation significantly overestimated the FPFR values for all the isotopologue pairs except the HD/H_2 from 50 to 300 K. And these deviations increase as the temperature decreases. However, for HD/H_2, an inversed deviation appears when the temperature is lower than ~150 K. This inversion can be explained by the nuclear-spin effect. The rotational contribution to the RPFR value of the HD/H_2 will be a temperature-independent constant as a result of the B-M equation due to the Teller-Redlich theorem (Redlich, 1935; Wilson et al., 1955), corresponds to a lnROT value of ~0.284. But if we take the nuclear-spin effect into account, the calculated lnROT value will be bigger than 0.284 when the temperature is low (e.g., lnROT = 0.6537 at 50 K in Table 5.1). Therefore, the RPFR/FPFR ratio of the HD/H_2 pair will be smaller than unity as the temperature decreases due to the nuclear-spin effect. In addition, we calculated the RPFR/FPFR ratios without including the DBOC effect. The results are shown in Fig. 5(b). After removing the DBOC effect, the deviations between the RPFR and FPFR values decreased but still can reach a very high value as ~30% for CH_3D/CH_4 pair. Therefore, except for the newly imported DBOC effect, other higher-order corrections such as vibrational anharmonicity, quantum mechanical rotation with nuclear-spin weights will still

Table 6
Calculated logarithms of the FPFR values of H_2, HF, HCl, HCN, H_2O, H_2S, NH_3, HCHO and CH_4 at 50–200 K.

T(K)	H_2	HF	HCl	HCN	H_2O	H_2S	NH_3	HCHO	NH_3	CH_4
50	8.7347	15.3984	11.7523	16.4353	17.0619	12.7941	18.1582	17.2473	18.1582	17.5010
60	7.2534	12.7781	9.7377	13.5654	14.1427	10.5829	15.0357	14.2579	15.0357	14.4772
70	6.1763	10.9063	8.2986	11.5155	12.0575	9.0035	12.8048	12.1226	12.8048	12.3169
80	5.3593	9.5024	7.2193	9.9780	10.4937	7.8190	11.1315	10.5211	11.1315	10.6966
90	4.7205	8.4104	6.3798	8.7824	9.2773	6.8976	9.8300	9.2755	9.8300	9.4363
100	4.2091	7.5368	5.7082	7.8260	8.3042	6.1606	8.7888	8.2791	8.7888	8.4281
110	3.7916	6.8220	5.1587	7.0438	7.5080	5.5575	7.9369	7.4638	7.9369	7.6033
120	3.4454	6.2263	4.7008	6.3923	6.8446	5.0550	7.2270	6.7844	7.2270	6.9159
130	3.1541	5.7223	4.3134	5.8414	6.2832	4.6298	6.6263	6.2095	6.6263	6.3343
140	2.9062	5.2902	3.9812	5.3698	5.8020	4.2654	6.1114	5.7168	6.1114	5.8358
150	2.6929	4.9158	3.6934	4.9617	5.3849	3.9495	5.6653	5.2897	5.6653	5.4038
160	2.5075	4.5881	3.4416	4.6053	5.0200	3.6732	5.2749	4.9161	5.2749	5.0258
170	2.3451	4.2990	3.2193	4.2914	4.6981	3.4293	4.9305	4.5865	4.9305	4.6923
180	2.2017	4.0421	3.0218	4.0131	4.4119	3.2126	4.6244	4.2935	4.6244	4.3958
190	2.0742	3.8121	2.8451	3.7648	4.1558	3.0188	4.3505	4.0315	4.3505	4.1307
200	1.9600	3.6052	2.6860	3.5419	3.9254	2.8444	4.1042	3.7957	4.1042	3.8921

Table 7
Calculated equilibrium constants compared with experimental values.

Reaction	T(K)	K (This work)	K (Urey model)	K (expt.)
$H_2 + D_2 = 2HD$	298	3.24	3.25	3.27 ± 0.02[a]
	200	2.87	2.85	
	100	2.22	1.91	
	50	1.28	0.86	
$H_2O + D_2O = 2HDO$	298	3.84	3.90	
	296	3.84	3.86	3.82 ± 0.06[b]
	273	3.81	3.83	3.74 ± 0.02[c]
	200	3.69	3.71	
	100	3.25	3.28	
	50	2.52	2.56	
$H_2S + D_2S = 2HDS$	297	3.89	3.92	3.88 ± 0.03[d]
	273	3.91	3.91	
	200	3.80	3.81	
	100	3.43	3.45	
	50	2.79	2.82	
$H_2O + HD = HDO + H_2$	297	3.43	3.58	3.46 ± 0.04[e]
	200	7.14	7.71	
	100	60.05	80.75	
	50	4135.02	8863.95	
$H_2O + HDS = HDO + H_2S$	273	2.22	2.34	2.28[f]
	300	2.06	2.17	2.10[f]
	200	2.95	3.18	
	100	8.53	9.92	
	50	71.36	96.59	
$NH_3 + NHD_2 = 2NH_2D$	298	2.97	2.92	2.92 ± 0.08[g]
	273	2.96	2.90	2.90 ± 0.06[g]
	200	2.91	2.83	
	100	2.71	2.55	
	50	2.34	2.07	

[a] Niki et al. (1965).
[b] Pyper and Christensen (1975).
[c] Friedman and Shiner (1966).
[d] Pyper and Newbury (1970).
[e] Bardo and Wolfsberg (1976).
[f] Richet et al. (1977).
[g] Pyper et al. (1967).

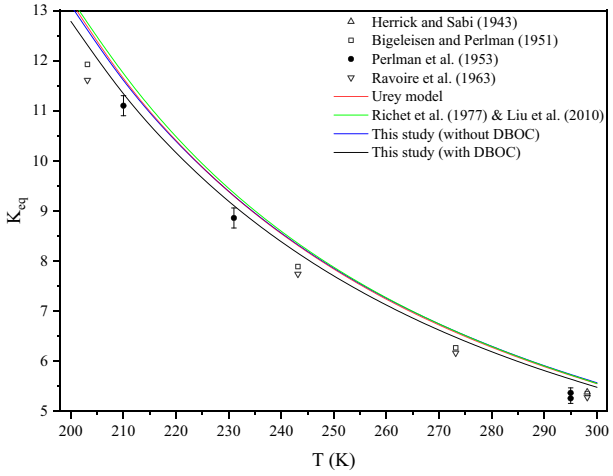

Fig. 4. Calculated and experimentally determined equilibrium constant for $NH_3 + HD = NH_2D + H_2$ from 200 to 300 K. The calculated values are showed as lines with different color using the same set of data.

drastically change the results, especially when the temperature is lower than 200 K.

Also, we calculated the relative differences between our results with the previously introduced modified B-M equation's results by Liu et al. (2010). To make difference with the B-M equation, the RPFR value calculated using the modified B-M equation is denoted as the CPFR (Corrected Partition Function Ratio: Liu et al., 2010). Because the method of Liu et al. (2010) can only be applied for non-linear molecules, we just performed our comparison for HDO/H_2O, HDS/H_2S, DCHO/HCHO, NH_2D/NH_3 and CH_3D/CH_4 pairs. The comparison results are shown in Fig. 6(a). Compared with the B-M equation, we can see that the method of Liu et al. (2010) do improve the results by including many higher-order corrections. And for the isotopologue pairs being compared here, almost all the relative differences decreased: HDO/H_2O (57.6% to 24.7%); HDS/H_2S (16.4% to 6.9%); DCHO/HCHO (5.8% to −11.2%); NH_2D/NH_3 (29.2% to 13.8%) and CH_3D/CH_4 (32.8% to 3.4%) at 50 K. Interestingly, when we remove the DBOC effect and recalculate the differences between our method and the method of Liu et al. (2010), both

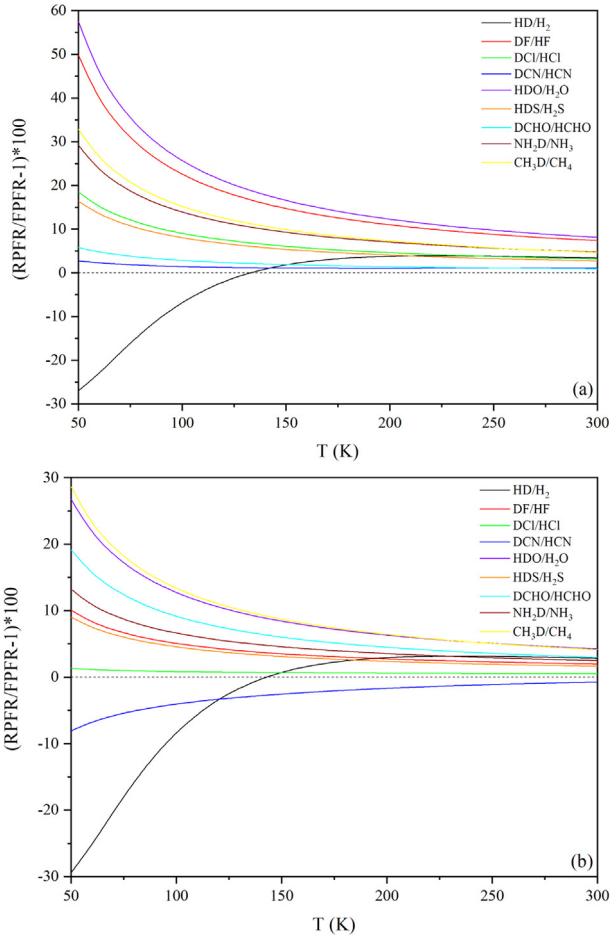

Fig. 5. Comparison of our calculated FPFR values with the RPFR values calculated using the B-M equation from 50 to 300 K. (a) The DBOC correction has been included. (b) The DBOC correction has been ignored.

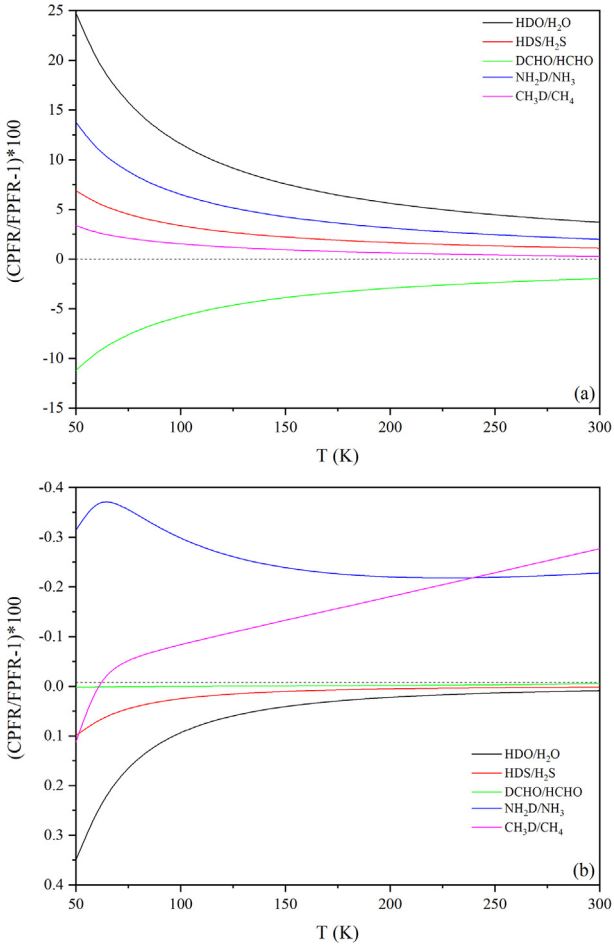

Fig. 6. Comparison of our calculated FPFR values with the CPFR values calculated using the method of Liu et al. (2010) from 50 to 300 K. (a) The DBOC correction has been included. (b) The DBOC correction has been ignored.

results are converged within 0.5% from 50 to 300 K (see Fig. 6(b)). Actually, this is a reasonable result because almost all the corrections we considered in this study have also been included in the modified B-M equation except for the nuclear-spin, inversion splitting and the DBOC effects. In addition, for these 5 isotopologue pairs, the nuclear-spin and inversion splitting effect are very small and can be ignored. Therefore, the big difference between Fig. 6(a) and 6(b) is a direct result of the DBOC, which also shows the necessity of including the DBOC into the calculations under low temperature conditions. In Fig. 6(b), the small difference between the FPFR and CPFR values (<0.5%) probably a result of the different equations used to describe those higher-order corrections.

As a result, the comparison confirms that the nuclear-spin and the DBOC effect are important and they should not be ignored at super-cold conditions.

5.3. The temperature dependence of FPFR under super-cold conditions

Using the results in Tables 5.1–5.9, we can evaluate the temperature dependence of all corrections (TRANS, ROT, VIB, CENTDIS, VIBROT and DB) under super-cold conditions. Taking the $HD + H_2O = HDO + H_2$ isotope exchange reaction as an example, Fig. 7 shows how each correction (except for the TRANS) changes with temperatures.

In general, $\ln\alpha_{TOTAL}$ is proportional to $1/T$ under super-cold conditions for the molecules investigated in the present study (Fig. 7(a)) rather than $1/T^2$ at high temperatures predicted by the B-M equation. The vibrational energy difference (VIB) accounts for most part of fractionations (Fig. 7(b)). This is just because the zero-point vibration energy difference dominates the fractionation at the super-cold conditions and $\ln\alpha_{TOTAL}$ approximately equals to $\frac{hc\Delta E_{ZPE}}{k_B}\cdot\frac{1}{T}$. Also, the contribution of the DBOC is also linearly proportional to the $1/T$ (Fig. 7(f)), which is easy to understand through Eq. (51). And $\ln\alpha_{ROT}$ is almost linearly proportional to the $1/T$ and no longer a temperature-independent constant as predicted by the B-M equation. This is because of the quantum effects of molecular rotation with nuclear-spin weights. We think the slow converging speed of the Q_{rot} for HD/H_2 pair can account for the minor non-linearity of $\ln\alpha_{ROT}$, which can often described by a polynomial series in previous works (Bigeleisen and Mayer, 1947; Richet et al., 1977). The vibration-rotational coupling (Fig. 7(d)) has minor contributions to $\ln\alpha_{TOTAL}$ ranges from −0.001 to 0.009. However, $\ln\alpha_{VIBROT}$ show a skewed raised relation to $1/T$, which has a minimum of ~0.009 at ~75 K. Finally, the centrifugal distortion (Fig. 7(e)) rapidly increases with the increasing of temperatures, which can be perfectly described by a cubic or quartic polynomial expression of $1/T$. As for the inversion splitting effect, from the calculated result of NH_2D/NH_3 (Table 5.8), we know that splitting of vibrational energy levels will significantly change the FPFR values at low temperatures, but the contribution of the splitting of rotational energy levels can be safely ignored.

5.4. DBOC for kinetic isotope fractionation in an elementary reaction

Except for equilibrium isotope effects, it is easy to infer that the DBOC correction will have significant effect on the reaction rate constant and therefore can change the kinetic isotope effect (KIE) too (e.g., combination reaction of H and H_2: Mielke et al., 2005). Here we use the thermal self-dissociation reaction of HCHO as an example to check this possibility (calculation details can be found in Supplementary file, Section S6). Its KIE in terms of D/H is controlled by these three reactions:

$$\text{H isotope}: \quad HCHO \overset{K_a}{\longleftrightarrow} [HCHO]^{TS} \xrightarrow{k_a} H_2 + CO \tag{a}$$

$$\text{D isotope}: \quad DCHO \overset{K_b}{\longleftrightarrow} [DCHO]^{TS} \xrightarrow{k_b} HD + CO \tag{b}$$

$$\text{D isotope}: \quad DCHO \overset{K_c}{\longleftrightarrow} [HCDO]^{TS} \xrightarrow{k_c} HD + CO \tag{c}$$

where the superscript TS means transition state. The KIE of $^{13}C/^{12}C$ is controlled by these two reactions:

$$^{12}C: H^{12}CHO \overset{K_d}{\longleftrightarrow} [H^{12}CHO]^{TS} \xrightarrow{k_d} H_{12} + {}^{12}CO \tag{d}$$

$$^{13}C: H^{13}CHO \overset{K_e}{\longleftrightarrow} [H^{13}CHO]^{TS} \xrightarrow{k_e} H_2 + {}^{13}CO \tag{e}$$

and the KIE of $^{18}O/^{16}O$ is controlled by these two reactions:

$$^{16}O: HCH^{16}O \overset{K_f}{\longleftrightarrow} [HCH^{16}O]^{TS} \xrightarrow{k_f} H_2 + C^{16}O \tag{f}$$

$$^{18}O: HCH^{18}O \overset{K_g}{\longleftrightarrow} [HCH^{18}O]^{TS} \xrightarrow{k_g} H_2 + C^{18}O \tag{g}$$

First, the geometry optimization and harmonic frequency analysis of the transition state $[HCHO]^{TS}$ is performed using the B3LYP/6-311+G(d, p) level (Krishnan et al., 1980; Becke, 1993; Schmidt et al., 1993) using the *Gaussian09* program. Only one imaginary vibration frequency is obtained after vibration analysis for the transition state. Then, the DBOC values of the HCHO and $[HCHO]^{TS}$ with their D-substituted isotopologues are calculated via *CFOUR* program at CCSD/aug-cc-pCVTZ level. Note that there are two different sites for H in the $[HCHO]^{TS}$, so the total correction factor K for the KIEs of D/H, $^{13}C/^{12}C$ and $^{18}O/^{16}O$ of this dissociation can be calculated by

$$K_H = \frac{K_b k_b + K_c k_c}{2K_a k_a} \tag{56}$$

$$K_C = \frac{K_e k_e}{K_d k_d} \tag{57}$$

$$K_O = \frac{K_g k_g}{K_f k_f} \tag{58}$$

The calculation results are listed in Table 8. It's obvious that the DBOC can significantly change the KIEs of the thermal self-dissociation reaction of HCHO by factors of 0.9745, 1.0027 and 1.0006 for D/H, $^{13}C/^{12}C$ and $^{18}O/^{16}O$ at 300 K, respectively. Their temperature dependences are also provided (Table 8). In addition, the effect due to the tunneling should also be considered. Mielke et al. (2005) showed that for $H + H_2$ reaction, the DBOC caused substantially larger barrier-height increases than tunneling.

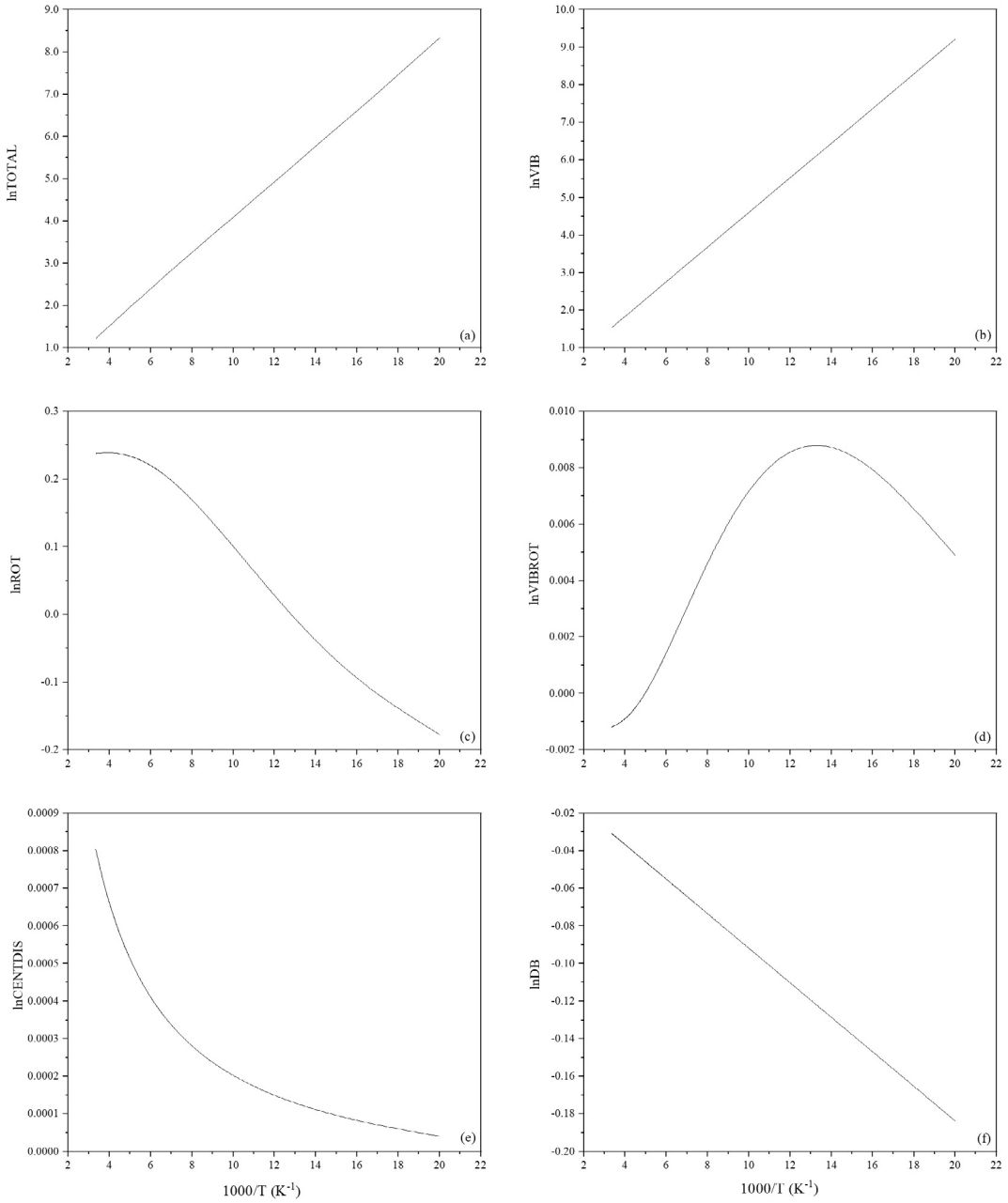

Fig. 7. Calculated corrections (logarithm values) and their temperature dependence of the $HD + H_2O = H_2 + HDO$ reaction at 50–300 K.

Table 8
Calculated DBOC correction factors for the KIEs of H/D, $^{13}C/^{12}C$, $^{18}O/^{16}O$ of the self-dissociation reaction of HCHO at different temperatures.

T(K)	K_H	K_C	K_O
300	0.9745	1.0027	1.0006
400	0.9808	1.0021	1.0004
500	0.9846	1.0016	1.0003
1000	0.9923	1.0008	1.0002
1500	0.9948	1.0005	1.0001
2000	0.9961	1.0004	1.0001

And for the $^{13}CH_4 + C_2H \rightarrow {}^{13}CH_3 + C_2H_2$ reaction, the DBOC and tunneling effect for its rate coefficient are 1.006 and 1.012 at 90 K (Nixon et al., 2012), respectively. Therefore, to obtain the KIEs with good accuracy under super-cold conditions, except for the DBOC effect, the effect of the quantum tunneling should also be included, which is beyond the scope of this study.

5.5. Potential broad applications of DBOC

From Tables 3a and 4, we can see that DBOC values for all the isotopologue pairs range from $-4.134\ cm^{-1}$

(DCHO/HCHO – D/H) to 10.716 cm^{-1} (DF/HF – D/H), corresponding to a factor from 1.1263 and 0.6900 at 50 K, respectively. An extreme case is that for an H/D exchange reaction between HF and HCHO, the H/D fractionation caused by DBOC (ΔE_{DBOC}(HF/HCHO) = 14.850 cm^{-1}) will be 0.9789 (−21.4 per mil) even at 1000 K. Table 4 shows the effect of DBOC for many organic molecules at ambient temperature. In addition, our comparison result in Fig. 4 shows that taking the DBOC effect into account can actually improve the accuracy of our calculations (At least for the H-D isotope exchange reaction between NH_3 and H_2). Therefore, the DBOC effect should be included at super-cold conditions at least for some systems.

The D/H ratio has become one of the most important issues for the evolution of the early solar system (e.g., Robert et al., 2000; Robert, 2010). However, the H/D fractionation behaviors are much more complex than we expected before. The temperatures of a common gas phase H/D isotopic exchange reaction in space are often <200 K (Robert, 2010), which means we need to treat H/D fractionations from a super-cold perspective, taking account of more quantum effects (e.g., nuclear-spin effect, inversion splitting and DBOC) and higher-order corrections (e.g., vibrational anharmonicity). However, the isotope exchange rate is extremely low so that it needs much longer time to reach isotope equilibrium, i.e., for D/H gas-phase exchange reaction between the H_2O and H_2, it needs ~2 Ma to reach equilibrium at 160 K (Lécluse and Robert, 1994). Therefore, the kinetic isotope effects are probably more important for such problems. Many studies (e.g., Aikawa et al., 2012; Nixon et al., 2012) used a time-dependent chemical model discussing the evolution of the D/H ratio for a proto solar-nebula or molecular clouds at low temperatures, these rate constants are crucial. However, theoretical calculations for these constants seldom consider this correction, which means that many theoretically calculated rate constants may be defective (e.g., Harding and Wagner, 1989; Karkach and Osherov, 1999; Corchado et al., 2000; Blitz et al., 2012; Meisner and Kästner, 2016). It may cause problems for works using a time-dependent chemical model which involving hundreds to thousands of isotopic exchange reactions for H/D systems at low temperatures, when try to explain the H/D ratio anomalies found by astronomical observations in the solar system (e.g., Aikawa et al., 2012; Nixon et al., 2012).

The DBOC also have effect on H/D systems at ambient temperatures according to our calculations (e.g., HF, HCl, CH_3OH and HCOOH). A previous study also showed that inclusion of the DBOC can greatly improve the accuracy of the calculated fractionation factor for the $D_2 + 2HCl = H_2 + 2DCl$ (Experimental value: 1.959 ± 0.011; Calculated with DBOC correction: 1.965; Calculated without DBOC correction: 2.017; T = 20 °C; Postma et al., 1988) reaction.

In addition, for other isotopic systems, such as $^{13}C/^{12}C$, $^{15}N/^{14}N$, $^{18}O/^{16}O$ and $^{34}S/^{32}S$, the DBOC corrections can also significantly change the fractionation factors, although to a smaller extent. From Eq. (55), we know that E_{DBOC} is proportional to the mass difference of the isotopologue pair AX_H/AX_L. As a result, the k_{DBOC} for the FPFR value will decrease as the increasing of the atomic mass. So the DBOC correction factors for C, N, O and S systems will become increasingly smaller. However, for these systems, this correction still can change the FPFR values to a very meaningful extent. Table 9 listed the DBOC correction factors for 12 gaseous molecules containing C, N, O and S, at 50–300 K. For $^{13}C/^{12}C$, $^{15}N/^{14}N$, $^{18}O/^{16}O$ and $^{34}S/^{32}S$ systems, the DBOC corrections will still cause a few per-mil fractionations at ambient temperatures and greater fractionations under super-cold conditions. Therefore, we suggest including the DBOC into H/D, $^{13}C/^{12}C$, $^{15}N/^{14}N$, $^{18}O/^{16}O$ and $^{34}S/^{32}S$ isotope fractionation calculations in future for ambient or lower temperatures.

Table 9
DBOC correction factors for 12 gaseous molecules containing C, N, O and S.

T(K)	$^{13}C/^{12}C$	$^{15}N/^{14}N$	$^{18}O/^{16}O$	$^{34}S/^{32}S$
Molecule	CH_4	NH_3	H_2O	H_2S
50	0.9783	0.9865	0.9868	0.9980
100	0.9891	0.9932	0.9934	0.9990
150	0.9927	0.9955	0.9956	0.9993
200	0.9945	0.9966	0.9967	0.9995
250	0.9956	0.9973	0.9974	0.9996
300	0.9963	0.9977	0.9978	0.9997
T(K)	$^{13}C/^{12}C$	$^{15}N/^{14}N$	$^{18}O/^{16}O$	$^{34}S/^{32}S$
Molecule	CO_2	*NNO	CO_2	SO_2
50	0.9815	0.9939	0.9927	0.9962
100	0.9907	0.9970	0.9964	0.9981
150	0.9938	0.9980	0.9976	0.9987
200	0.9953	0.9985	0.9982	0.9990
250	0.9963	0.9988	0.9985	0.9992
300	0.9969	0.9990	0.9988	0.9994
T(K)	$^{13}C/^{12}C$	$^{15}N/^{14}N$	$^{18}O/^{16}O$	$^{34}S/^{32}S$
Molecule	HCN	N*NO	SO_3	SO_3
50	0.9875	0.9887	0.9957	0.9901
100	0.9937	0.9943	0.9978	0.9950
150	0.9958	0.9962	0.9986	0.9967
200	0.9969	0.9972	0.9989	0.9975
250	0.9975	0.9977	0.9991	0.9980
300	0.9979	0.9981	0.9993	0.9983

5.6. Nuclear-spin effect for H_2

We assume that the all the spin-isomers of H_2 are in thermal equilibrium when calculating its Q_{rot}, which means that the ratio *ortho*/*para*- H_2 is always 3:1 (The high-temperature limit). However, the transitions between the two spin-isomers are very slow and often take a long time (Flower et al., 2006), let alone at super-cold conditions. Therefore, we evaluated the effect of different *ortho*/*para* ratio (denoted as *o*/*p* ratio hereafter) on the final calculated FPFR value of HD/H_2 pair from 50 to 300 K.

We calculated the logarithm of the Q_{rot} ratio of the HD/H_2 pair with different *o*/*p* ratios range from 0 (all H_2 molecules are *para*-H_2) to infinite (all H_2 molecules are *ortho*-H_2). The results are shown in Fig. 8. We find that the effect of different *o*/*p* (*ortho*/*para*) ratios rapidly decreases when temperature increases. When temperature is 250 K, the calculated logarithm of the Q_{rot} ratio changes from 0.2658 to 0.2488 and when the temperature is higher,

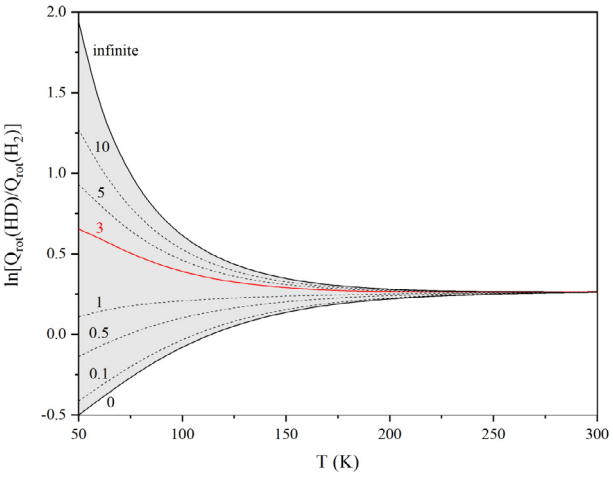

Fig. 8. Calculated logarithms of the Q_{rot} ratio of the HD/H_2 pair with different *ortho*/*para* ratio (ranges from 0 to infinite) at 50–300 K.

this interval becomes smaller. However, when the temperature is 50 K, this interval increases, and the calculated ratio changes from −0.5006 to 1.9412. Interestingly, the calculated Q_{rot} ratios are positively correlated with the o/p ratios. When the o/p ratios are relatively small (e.g., <0.5) and the temperatures are also very low (e.g., <100 K), the corresponding Q_{rot} ratios will be smaller than unity, which means that the isotope effect caused by molecular rotation will show an inversed effect on the isotope fractionations when compared with the Urey model. Light isotopes will be enriched rather than heavy isotopes due to the molecular rotation at such conditions.

For other molecules such as CH_4, NH_3 and H_2O, we think that whether their spin-isomers are in thermal equilibrium or not, the effect of this kind of disequilibrium on the fractionation can be ignored. Because the nuclear-spin effect of these molecules only become significant when the temperatures are lower than 50 K, which is beyond our considerations. In addition, the true distribution of spin-isomers of these molecules are much more difficult to evaluate than a simple diatomic molecule or H_2O (Can be easily discussed by using the o/p ratio) when thermal equilibrium is not reached. Therefore, we only evaluated the effect of o/p ratios for H_2 here and the final calculated FPFR values are based on the equilibrated o/p ratio (3:1). The equilibrium fractionation factors involving other o/p ratios for H_2 can be easily determined by using the Eq. (18).

5.7. Limitations of our method and future work

There are still some limitations in our method built for the super-cold conditions:

(1) Our method is applied to systems where the intermolecular forces can be ignored (i.e., a dilute gas system), and for those processes that quantum tunneling effect can be ignored. In addition, a relatively stable environment with a long stagnation time (at least ~ 1 Ma) is needed.

(2) Extending our theory to solid systems seems natural due to the success of the statistic mechanics for solids. However, to our knowledge, there is no packages can evaluate the DBOC for solids although the theory of the DBOC has been built for decades. Perhaps the DBOC for solids can be evaluated using a cluster model instead.

(3) Accurate calculation of the DBOC require an accurate description of the wavefunctions and their second derivatives relative to the nuclear coordinates, which is often too expensive (e.g., a CCSD/aug-cc-pCVTZ or higher level calculations) to afford for large molecules. Although there have been studies using semi-empirical or density functional theory (DFT) methods to deal with it, the results are still dissatisfactory (Mohallem, 2008; Gidopoulos and Gross, 2014). Also, the classic method such as an asymptotic expansion of the DBOC might also help sometimes (Przybytek and Jeziorski, 2012). Therefore, affordable methods are needed to fulfill the calculation of DBOC for large systems.

(4) The DBOC is calculated with the precondition of higher order non-adiabatic corrections on Born-Oppenheimer approximation are small and nearly cancelled when comparing the energy differences of isotopologue pairs (Kleinman and Wolfsberg, 1973). Therefore, these higher-order non-adiabatic corrections possibly still need to be checked in the future for safe.

6. CONCLUSIONS

We build a theoretical method to calculate isotope fractionations under super-cold conditions. The isotope fractionation behaviors of such conditions are found to be quite different from those at higher temperatures, such as the logarithm of equilibrium fractionation factors is proportional to $1/T$ (for all the molecules been studied here) rather than $1/T^2$. The fractionation behavior of isotopes (H, C, N, O, S and other light elements) are mainly dominated by the vibrational energy differences (including the vibrational anharmonicity). The rotational (quantum mechanical rotation including the nuclear-spin weight), translational (temperature-independent) and the electronic energy differences (DBOC) can also affect the results to a very meaningful extent. Other higher-order corrections (such as the vibration-rotational coupling, centrifugal distortion and inversion splitting) can only provide trivial effects.

The effect of the nuclear-spin on the isotope fractionation is significant under super-cold conditions, especially for those molecules have wider rotational energy intervals such as H_2 and its isotopologues HD and D_2. However, this effect will rapidly vanish with increasing temperature.

The DBOC is a very important effect for isotope fractionations even at ambient temperatures. It is also important for kinetic isotope fractionation of elementary reactions. However, this effect becomes increasingly smaller with the order of H, C, O, N and S isotope systems. This

study has provided a lot of isotope fractionation factors for gaseous molecules and organic molecules with the consideration of the DBOC. The magnitudes of the DBOC corrections are beyond our expectation and it will become a very important effect in future isotope fractionation calculations.

ACKNOWLEDGEMENTS

Y.L. is grateful for funding supports from the strategic priority research program (B) of CAS (XDB18010100), 973 Program (2014CB440904) and Chinese NSF projects (41530210, 41490635, 41225012). We thank Qi Liu (CAS), Huiming Bao, Xiaobin Cao and Yuyang He at Louisiana State University for helpful discussions. And we also thank Dr. Daniel L. Eldridge and the other two anonymous reviewers for their very helpful comments that improved our manuscript. All the calculations of this work are performed at TianHe-2 supercomputer.

REFERENCES

Aikawa Y., Wakelam V., Hersant F., Garrod R. T. and Herbst E. (2012) From prestellar to protostellar cores. II. Time dependence and deuterium fractionation. *Astrophys. J.* **760**, 40–58.

Altwegg K., Balsiger H., Bar-Nun A., Berthelier J. J., Bieler A., Bochsler P., Briois C., Calmonte U., Combi M., De Keyser J., Eberhardt P., Fiethe B., Fuselier S., Gasc S., Gombosi T. I., Hansen K. C., Hässig M., Jäckel A., Kopp E., Korth A., LeRoy L., Mall U., Marty B., Mousis O., Neefs E., Owen T., Rème H., Rubin M., Sémon T., Tzou C. Y., Waite H. and Wurz P. (2014) 67P/Churyumov-Gerasimenko, a Jupiter family comet with a high D/H ratio. *Science* **347**, 1261952.

Arrighini G. P. and Guidotti C. (1995) The rotational partition function of diatomic molecules. *Mol. Phys.* **86**, 1299–1305.

Azzam A. A. A., Tennyson J., Yurchenko S. N. and Naumenko O. V. (2016) ExoMol molecular line lists-XVI. The rotation-vibration spectrum of hot H_2S. *MNRAS* **460**, 4063–4074.

Bardo R. D., Kleinman L. I., Raczkowski A. W. and Wolfsberg M. (1978) The effects of electron correlation on the adiabatic correction and on equilibrium constants for isotopic exchange reactions. *J. Chem. Phys.* **69**, 1106–1111.

Bardo R. D. and Wolfsberg M. (1975) The nuclear mass dependence of the adiabatic correction to the Born-Oppenheimer approximation. *J. Chem. Phys.* **62**, 4555–4558.

Bardo R. D. and Wolfsberg M. (1976) A theoretical calculation of the equilibrium constants for the isotopic exchange reaction between H_2O and HD. *J. Phys. Chem.* **80**, 1068–1071.

Bardo R. D. and Wolfsberg M. (1977) The wave equation of a nonlinear triatomic molecule and the adiabatic correction to the Born-Oppenheimer approximation. *J. Chem. Phys.* **67**, 593–603.

Bardo R. D. and Wolfsberg M. (1978) The adiabatic correction for nonlinear triatomic molecules: Techniques and calculations. *J. Chem. Phys.* **68**, 2686–2695.

Barone V. (2004) Vibrational zero-point energies and thermodynamic functions beyond the harmonic approximation. *J. Chem. Phys.* **120**, 3059–3065.

Barone V. (2005) Anharmonic vibrational properties by a fully automated second-order perturbative approach. *J. Chem. Phys.* **122**, 014108.

Barone V. and Minichino C. (1995) From concepts to algorithms for the treatment of large amplitude internal motions and unimolecular reactions. *J. Mol. Struct.* **330**, 365–376.

Becke A. D. (1993) Density-functional thermochemistry. III. The role of exact exchange. *J. Chem. Phys.* **98**, 5648–5652.

Benedict W. S. and Plyler E. K. (1956) Interaction of stretching vibrations and inversion in ammonia. *J. Chem. Phys.* **24**, 904.

Bigeleisen J. (1996) Nuclear size and shape effects in chemical reactions. Isotope chemistry of the heavy elements. *J. Am. Chem. Soc.* **118**, 3676–3680.

Bigeleisen J. and Mayer M. G. (1947) Calculation of equilibrium constants for isotopic exchange reactions. *J. Chem. Phys.* **15**, 261–267.

Bigeleisen J. and Perlman M. L. (1951) *The concentration of deuterium by chemical exchange between hydrogen and ammonia*. Brookhaven National Lab, Upton, NY.

Blitz M. A., Talbi D., Seakins P. W. and Smith W. M. (2012) Rate constants and branching ratios for the reaction of CH radicals with NH_3: A combined experimental and theoretical study. *J. Phys. Chem. A.* **116**, 5877–5885.

Bomble Y. J., Vázquez J., Kállay M., Michauk C., Szalay P. G., Császár A. G., Gauss J. and Stanton J. F. (2006) High-accuracy extrapolated ab initio thermochemistry. II. Minor improvements to the protocol and a viral simplification. *J. Chem. Phys.* **125**, 064108.

Born J. and Wolfsberg M. (1972) Effect of vibrational anharmonicity on hydrogen-deuterium exchange equilibria involving ammonia molecules. *J. Chem. Phys.* **57**, 2862–2869.

Born K. and Huang K. (1956) *Dynamical Theory of Crystal Lattices*. Oxford University, New York.

Bron J. (1974) Zero-point energy of linear triatomic molecules. *J. Chem. Soc., Faraday Trans.* **70**, 871–874.

Bubin S. and Adamowicz L. (2007) Calculations of the ground states of BeH and BeH^+ without the Born-Oppenheimer approximation. *J. Chem. Phys.* **126**, 214305.

CFOUR, Coupled-Cluster techniques for Computational Chemistry, a quantum-chemical program package by J. F. Stanton, J. Gauss, L. Cheng, M. E. Harding, D. A. Matthews, P. G. Szalay with contributions from A. A. Auer, R. J. Bartlett, U. Benedikt, C. Berger, D. E. Bernholdt, Y. J. Bomble, O. Christiansen, F. Engel, R. Faber, M. Heckert, O. Heun, M. Hilgenberg, C. Huber, T.-C. Jagau, D. Jonsson, J. Jusélius, T. Kirsch, K. Klein, W.J. Lauderdale, F. Lipparini, T. Metzroth, L. A. Mück, D. P. O'Neill, D. R. Price, E. Prochnow, C. Puzzarini, K. Ruud, F. Schiffmann, W. Schwalbach, C. Simmons, S. Stopkowicz, A. Tajti, J. Vázquez, F. Wang, J. D. Watts and the integral packages MOLECULE by J. Almlöf and P. R. Taylor, PROPS by P. R. Taylor, ABACUS by T. Helgaker, H. J. Aa. Jensen, P. Jørgensen, and J. Olsen, and ECP routines by A. V. Mitin and C. van Wüllen. For the current version, see http://www.cfour.de.

Chakraborty S., Muskatel B. H., Jackson T. L., Ahmed M., Levine R. D. and Thiemens M. H. (2014) Massive isotopic effect in vaccum UV photodissociation of N_2 and implications for meteorite data. *Proc. Nat. Acad. Sci. U.S.A.* **111**, 14704–14709.

Cohen M. J., Handy N. C., Hernandez R. and Miller W. H. (1992) Cumulative reaction probabilities for $H + H_2 \rightarrow H_2 + H$ from a knowledge of the anharmonic force field. *Chem. Phys. Lett.* **192**, 407–416.

Corchado J. C., Truhlar D. G. and Espinosa-Garćia J. (2000) Potential energy surface, thermal, and state-selected rate coefficients, and kinetic isotope effect for $Cl + CH_4 \rightarrow HCl + CH_3$. *J. Chem. Phys.* **112**, 9375–9389.

Cordier D., Mousis O., Lunine J. I., Moudens A. and Vutton V. (2008) Photochemical enrichment of deuterium in Titan's atmosphere: new insights from *CASSINI-HUYGENS*. *Astrophys. J.* **689**, L61–L64.

Dennison, D. M., Hecht, K. T. (1962) Molecular spectra. Quantum Theory. Quantum Theory, Part II: Aggregates of Particles.

Dunning, Jr., T. H. (1989) Gaussian basis sets for use in correlated molecular calculations. I. The atoms boron through neon and hydrogen. *J. Chem. Phys.* **90**, 1007–1023.

Eberhardt P., Dolder U., Schulte W., Krankowsky D., Lämmerzahl P., Hoffman J. H., Hodges R. R., Berthelier J. J. and Illiano J. M. (1987) The D/H ratio in water from comet P/Halley. *Astron. Astrophys.* **187**, 435–437.

Flower D. R., Forêts G. P. and Walmsley C. M. (2006) The importance of the ortho:para H_2 ratio for the deuteration of molecules during pre-protostellar collapse. *Astron. Astrophys.* **449**, 621–629.

Fox K. (1970) On the rotational partition function for tetrahedral molecules. *J. Quant. Spectrosc. Radiat. Transfer.* **10**, 1335–1342.

Friedman L. and Shiner V. J. (1966) Experimental determination of disproportionation of hydrogen isotopes in water. *J. Chem. Phys.* **44**, 4639–4640.

Frisch M. J., Trucks G. W., Schlegel H. B., Scuseria G. E., Robb M. A., Cheeseman J. R., Scalmani G., Barone V., Mennucci B., Petersson G. A., Nakatsuji H., Caricato M., Li X., Hratchian H. P., Izmaylov A. F., Bloino J., Zheng G., Sonnenberg J. L., Hada M., Ehara M., Toyota K., Fukuda R., Hasegawa J., Ishida M., Nakajima T., Honda Y., Kitao O., Nakai H., Vreven T., Montgomery, Jr., J. A., Peralta J. E., Ogliaro F., Bearpark M., Heyd J. J., Brothers E., Kudin K. N., Staroverov V. N., Kobayashi R., Normand J., Raghavachari K., Rendell A., Burant J. C., Iyengar S. S., Tomasi J., Cossi M., Rega N., Millam J. M., Klene M., Knox J. E., Cross J. B., Bakken V., Adamo C., Jaramillo J., Gomperts R., Stratmann R. E., Yazyev O., Austin A. J., Cammi R., Pomelli C., Ochterski J. W., Martin R. L., Morokuma K., Zakrzewski V. G., Voth G. A., Salvador P., Dannenberg J. J., Dapprich S., Daniels A. D., Farkas Ö., Foresman J. B., Ortiz J. V., Cioslowski J. and Fox D. J. (2009) *Gaussian 09*. Gaussian Inc, Wallingford CT.

Fujii T., Moynier F. and Albarède F. (2009) The nuclear field shift in chemical exchange reactions. *Chem. Geol.* **267**, 139–156.

Fujii Y., Nomura M., Okamoto M., Onitsuka H., Kawakami H. and Takeda K. (1989) An anomalous isotope effect of ^{235}U in U(IV)-U(VI) chemical exchange. *Z. Naturforsch.* **44**, 395–398.

Gauss J., Tajti A., Kállay M., Stanton J. F. and Szalay P. G. (2006) Analytic calculation of the diagonal Born-Oppenheimer correction within configuration-interaction and coupled-cluster theory. *J. Chem. Phys.* **125**, 144111.

Gidopoulos N. I. and Gross E. K. U. (2014) Electronic non-adiabatic states: towards a density functional theory beyond the Born-Oppenheimer approximation. *Phil. Trans. R. Soc. A.* **372**, 20130059.

Goncalves C. P. and Mohallem J. R. (2003) Self-consistent-field - Hartree-Fock method with finite nuclear mass corrections. *Theor. Chem. Acc.* **110**, 367–370.

Handy N. C., Yamaguchi Y. and Schaefer H. F. (1986) The diagonal correction to the Born-Oppenheimer approximation: Its effect on the singlet-triplet splitting of CH_2 and other molecular effects. *J. Chem. Phys.* **84**, 4481–4484.

Harding L. B. and Wagner A. F. (1989) Theoretical study of the reaction rates of OH + OH ↔ H_2O + O. *Symposium (International) on Combustion* **22**, 983–989.

Harding M. E., Metzroth T. and Gauss J. (2008a) Parallel calculation of CCSD and CCSD(T) analytic first and second derivatives. *J. Chem. Theory Comput.* **4**, 64–74.

Harding M. E., Vázquez J., Ruscic B., Wilson A. K., Gauss J. and Stanton J. F. (2008b) High-accuracy extrapolated ab initio thermochemistry. III. Additional improvements and overview. *J. Chem. Phys.* **128**, 114111.

Herrick C. E. and Sabi N. S. A. M. (1943) Columbia University Secret Report A-765.

Herzberg G. (1945) *Molecular Spectra and Molecular Structure. II. Infrared and Raman Spectra of Polyatomic Molecules*. Van Nostrand, Princeton.

Holka F., Szalay P. G., Fremont J., Rey M., Peterson K. A. and Tryterev V. G. (2011) Accurate ab initio determination of the adiabatic potential energy function and the Born-Oppenheimer breakdown corrections for the electronic ground state of LiH isotopologues. *J. Chem. Phys.* **134**, 094306.

Imafuku Y., Minori Ab, Schmidt M. W. and Hada M. (2016) Heavy element effects in the diagonal Born-Oppenheimer correction within a relativistic spin-free Hamiltonian. *J. Phys. Chem. A* **120**, 2150–2159.

Ioannou A. G., Amos R. D. and Handy N. C. (1996) The diagonal Born-Oppenheimer correction for He_2^+ and F + H_2. *Chem. Phys. Letts.* **251**, 52–58.

Isaacson A. D. (2002) Anharmonic effects on the transition state theory rate constant. *J. Chem. Phys.* **117**, 8778–8786.

Isaacson A. D. (2006) Including anharmonicity in the calculation of rate constants. 1. The HCN/HNC isomerization reaction. *J. Phys. Chem. A* **110**, 379–388.

Jansen S., Ruskai M. B. and Seiler R. (2007) Bounds for the adiabatic approximation with applications to quantum computation. *J. Math. Phys.* **48** 102111.

Karkach S. P. and Osherov V. I. (1999) Ab initio analysis of the transition states on the lowest triplet H_2O_2 potential surface. *J. Chem. Phys.* **110**, 11918–11927.

Karton A., Ruscic B. and Martin J. M. L. (2007) Benchmark atomization energy of ethane: Importance of accurate zero-point vibrational energies and diagonal Born-Oppenheimer corrections for a 'simple' organic molecule. *J. Mol. Struct.* **811**, 345–353.

Kivelson D. and Wilson, Jr., E. B. (1952) Approximated treatment of the effect of centrifugal distortion on the rotational energy levels of asymmetric rotor molecules. *J. Chem. Phys.* **20**, 1575–1579.

Kleinman L. I. and Wolfsberg M. (1973) Corrections to the Born-Oppenheimer approximation and electronic effects on isotopic exchange equilibria. *J. Chem. Phys.* **59**, 2043–2053.

Kleinman L. I. and Wolfsberg M. (1974a) Corrections to the Born-Oppenheimer approximation and electronic effects on isotopic exchange equilibria. II. *J. Chem. Phys.* **60**, 4740–4748.

Kleinman L. I. and Wolfsberg M. (1974b) Shifts in vibrational constants from corrections to the Born-Oppenheimer approximation: Effects on isotopic exchange equilibria. *J. Chem. Phys.* **60**, 4749–4754.

Krishnan R., Binkely J. S., Seeger R. and Pople J. A. (1980) Self-consistent molecular orbital methods. XX. A basis set for correlated wave functions. *J. Chem. Phys.* **72**, 650–654.

Lécluse C. and Robert F. (1994) Hydrogen isotope exchange reaction rates: Origin of water in the inner solar system. *Geochim. Cosmochim. Acta* **58**, 2927–2939.

Liévin J., Demaison J., Herman M., Fayt A. and Puzzarini C. (2011) Comparison of the experimental, semi-experimental and ab initio equilibrium structures of acetylene: influence of relativistic effects and of the diagonal Born-Oppenheimer corrections. *J. Chem. Phys.* **134**, 064119.

Liu Q., Tossell J. A. and Liu Y. (2010) On the proper use of the Bigeleisen-Mayer equation and corrections to it in the calculation of isotopic fractionation equilibrium constants. *Geochim. Cosmochim. Acta* **74**, 6965–6983.

Lutz J. J. and Hutson J. M. (2016) Deviations from Born-Oppenheimer mass scaling in spectroscopy and ultracold molecular physics. *J. Mol. Spectrosc.* **330**, 43–56.

Martin J. M. L., Francois P. J. and Gijbels R. (1991) On the effect of centrifugal stretching on the rotational partition function of an asymmetric top. *J. Chem. Phys.* **95**, 8374–8389.

McDowell R. S. (1987) Rotational partition functions for spherical-top molecules. *J. Quant. Spectrosc. Radiat. Transfer.* **38**, 337–346.

McDowell R. S. (1988) Rotational partition functions for linear molecules. *J. Chem. Phys.* **88**, 356–361.

McDowell R. S. (1990) Rotational partition functions for symmetric-top molecules. *J. Chem. Phys.* **93**, 2801–2811.

Mead C. A. and Truhlar D. G. (1979) On the determination of Born-Oppenheimer nuclear motion wave functions including complications due to conical intersections and identical nuclei. *J. Chem. Phys.* **70**, 2284–2296.

Meisner J. and Kästner J. (2016) Reaction rates and kinetic isotope effects of H_2 + OH → H_2O +H. *J. Chem. Phys.* **144**, 174303.

Mielke S. L., Schwenke D. W. and Peterson K. A. (2005) Benchmark calculations of the complete configuration-interaction limit of Born-Oppenheimer diagonal corrections to the saddle points of isotopomers of the H + H_2 reaction. *J. Chem. Phys.* **122**, 224313.

Mielke S. L., Schwenke D. W., Schatz G. C., Garrett B. C. and Peterson K. A. (2009) Functional representation for the Born-Oppenheimer diagonal correction and Born-Huang adiabatic potential energy surfaces for isotopomers of H_3^+. *J. Phys. Chem. A.* **113**, 4479–4488.

Møller C. and Plesset M. S. (1934) Note on an approximation treatment for many-electron systems. *Phys. Rev.* **46**, 618–622.

Mohallem J. R. (2008) Semiempirical evaluation of post-Hartree-Fock diagonal-Born-Oppenheimer corrections for organic molecules. *J. Chem. Phys.* **128**, 144113.

Niki H., Rousseau Y. and Mains G. J. (1965) They hydrogen-deuterium exchange reaction. I. 6^3P_1 mercury photosensitized. *J. Phys. Chem.* **69**, 45–52.

Nixon C. A., Temelso B., Vinatier S., Teanby N. A., Bézard B., Achterberg R. K., Mandt K. E., Sherrill C. D., Irwin P. G., Jenning D. E., Romani P. N., Coustenis A. and Flasar F. M. (2012) Isotopic ratios in Titan's methane: measurements and modeling. *Astrophys. J.* **749**, 159–173.

Nomura M., Higuchi N. and Fujii Y. (1996) Mass dependence of uranium isotope effects in the U(IV)-U(VI) exchange reaction. *J. Am. Chem. Soc.* **118**, 9127–9130.

Pachucki K. and Komasa J. (2008) Nonadiabatic corrections to the wave function and energy. *J. Chem. Phys.* **129**, 034102.

Pachucki K. and Komasa J. (2009) Nonadiabatic corrections to rovibrational levels of H_2. *J. Chem. Phys.* **130**, 164113.

Pennington R. E. and Kobe K. A. (1954) Contributions of vibrational anharmonictiy and rotation-vibration interaction to thermodynamic functions. *J. Chem. Phys.* **22**, 1442–1447.

Perlman M., Bigeleisen J. and Elliott N. (1953) Equilibrium in the exchange of deuterium between ammonia and hydrogen. *J. Chem. Phys.* **21**, 70–72.

Peterson K. A. and Dunning T. H. (2002) Accurate correlation consistent basis sets for molecular core-valence correlation effects: The second row atoms Al-Ar, and the first row atoms B-Ne revisited. *J. Chem. Phys.* **117**, 10548–10560.

Pfeiffer F., Rauhut G., Feller D. and Peterson K. A. (2013) Anharmonic zero point vibrational energies: Tipping the scales in accurate thermochemistry calculations? *J. Chem. Phys.* **138**, 044311.

Piccardo M., Bloino J. and Barone V. (2015) Generalized vibrational perturbation theory for rotovibrational energies of linear, symmetric and asymmetric tops: Theory, approximations, and automated approaches to deal with medium-to-large molecular systems. *Int. J. Quantum Chem.* **115**, 948–982.

Pinto J. P., Lunine J. I., Kim S. J. and Yung Y. L. (1986) D to H ratio and the origin and evolution of Titan's atmosphere. *Nature* **319**, 388–390.

Pliva J. (1990) Anharmonic constants for degenerate modes of symmetric top molecules. *J. Mol. Spectrosc.* **139**, 278–285.

Postma J. M., Silvester L. F. and Rock P. A. (1988) Thermodynamics of hydrogen-isotope-exchange reaction. 3. An experimental test of the Born-Oppenheimer approximation. *J. Phys. Chem.* **92**, 1308–1312.

Przybytek M. and Jeziorski B. (2012) Long-range asymptotic expansion of the diagonal Born-Oppenheimer correction. *Chem. Phys.* **401**, 170–179.

Pyper J. W. and Christensen L. D. (1975) Equilibrium constants of hydrogen-deuterium-tritium self-exchange reactons in water vapor as studied with a pulsed molecular-beam quadrupole mass filter. *J. Chem. Phys.* **62**, 2596–2599.

Pyper J. W. and Newbury R. S. (1970) Hydrogen-deuterium self-exchange in hydrogen sulfide and hydrogen selenide as studied with a pulsed-molecular-beam quadrupole mass filter. *J. Chem. Phys.* **52**, 1966–1971.

Pyper J. W., Newbury R. S. and Barton G. W. (1967) Study of the isotopic disproportionation reaction between light and heavy water using a pulsed-molecular-beam mass spectrometer. *J. Chem. Phys.* **46**, 2253–2257.

Ravoire J., Grandcollot P. and Dirian G. (1963) Determination of the separation factor of deuterium between ammonia and hydrogen. *J. Chim. Phys.* **60**, 130.

Redlich O. (1935) Eine allgemeine beziehung zwischen den schwingungsfrequenzen isotoper molekeln. *Z. Phys. Chem. B.* **28**, 371–382.

Richet P., Bottinga Y. and Javoy M. (1977) A review of hydrogen, carbon, nitrogen, oxygen, sulphur, and chlorine stable isotope fractionation among gaseous molecules. *Ann. Rev. Earth Planet. Sci.* **5**, 65–110.

Robert F. (2010) Solar system deuterium/hydrogen ratio. *Meteorite Early Sol. Syst. II*, 341–351.

Robert F., Gautier D. and Dubrulle B. (2000) The solar system D/H ratio: observations and theories. *Space Sci. Rev.* **92**, 201–224.

Schauble E. A. (2004) Applying stable isotope fractionation theory to new systems. *Rev. Mineral. Geochem.* **55**, 65–111.

Schauble E. A. (2007) Role of nuclear volume in driving equilibrium stable isotope fractionation of mercury, thallium and other very heavy elements. *Geochim. Cosmochim. Acta* **71**, 2170–2189.

Schauble E. A. (2013) Modeling nuclear volume isotope effects in crystals. *Proc. Nat. Acad. Sci. U.S.A.* **110**, 17714–17719.

Schmidt M. W., Baldridge K. K., Boatz J. A., Elbert S. T., Gordon M. S., Jensen J. H., Koseki S., Matsunaga N., Nguyen K. A., Su S. J., Windus T. L., Dupuis M. and Montgomery J. A. (1993) General atomic and molecular electronic-structure system. *J. Comput. Chem.* **14**, 1347–1363.

Schuurman M. S., Allen W. D. and Schaefer H. F. (2005) The *ab initio* limit quartic force field of BH_3. *J. Comput. Chem.* **26**, 1106–1112.

Schwartz C. and Le Roy R. J. (1987) Nonadiabatic eigenvalues and adiabatic matrix elements for all isotopes of diatomic hydrogen. *J. Mol. Spectrosc.* **121**, 420–439.

Shaffer W. H. (1941) Rotation-vibration energies of the pyramidal XY_3 molecular model. *J. Chem. Phys.* **9**, 607–615.

Shaffer W. H. and Schuman R. P. (1944) The infra-red spectra of bent XYZ molecules part I. Vibration-rotation energies. *J. Chem. Phys.* **12**, 504–513.

Snels M., Hollenstein H. and Quack M. (2006) Mode selective tunneling dynamics observed by high resolution spectroscopy of the bending fundamentals of $^{14}NH_2D$ and $^{14}ND_2H$. *J. Chem. Phys.* **125**, 194319.

Tajti A., Szalay P. G., Császár A. G., Kállay M., Gauss J., Valeev E. F., Flowers B. A., Vázquez J. and Stanton J. (2004) HEAT: High accuracy extrapolated ab initio thermochemistry. *J. Chem. Phys.* **121**, 11599–11613.

Tajti A., Szalay P. G. and Gauss J. (2007) Perturbative treatment of the electron-correlation contribution to the diagonal Born-Oppenheimer correction. *J. Chem. Phys.* **127**, 014102.

Tennyson J., Zobov N. F., Williamson R., Polyansky O. L. and Bernath P. F. (2001) Experimental energy levels of the water molecule. *J. Phys. Chem. Ref. Data.* **30**, 735–830.

Truhlar D. G. and Isaacson A. D. (1991) Simple perturbation theory estimates of equilibrium constants from force fields. *J. Chem. Phys.* **94**, 357–359.

Tubman N. M., Kylänpää I., Schiffer S. H. and Ceperley D. M. (2014) Beyond the Born-Oppenheimer approximation with quantum Monte Carlo methods. *Phys. Rev. A.* **90**, 042507.

Urey H. C. (1947) The thermodynamic properties of isotopic substances. *J. Chem. Soc. (Lond.)*, 562–581.

Valeev E. F. and Sherrill C. D. (2003) The diagonal Born-Oppenheimer correction beyond the Hartree-Fock approximation. *J. Chem. Phys.* **118**, 3921–3927.

Vázquez J. and Stanton J. (2006) Simple(r) algebraic equation for transition moments of fundamental transitions in vibrational second-order perturbation theory. *Mol. Phys.* **104**, 377–388.

Voronin B. A., Tennyson J., Tolchenov R. N., Lugovskoy A. A. and Yurcheno S. N. (2010) A high accuracy computed line list for the HDO molecule. *Mon. Not. R. Astron. Soc.* **402**, 492–496.

Watson J. K. (1968) Determination of centrifugal distortion coefficients of asymmetric top molecules. III. Sextic coefficients. *J. Chem. Phys.* **48**, 181–185.

Watson J. K. G. (1988) The asymptotic asymmetric-top rotational partition function. *Mol. Phys.* **65**, 1377–1397.

Webster C. R., Mahaffy P. R., Flesch G. J., Niles P. B., Jones J. H., Leshin L. A., Atreya S. K., Stern J. C., Christensen L. E., Owen T., Franz H., Pepin R. O. and Steele A.the MSL Science Team (2013) Isotope ratios of H, C, and O in CO_2 and H_2O of the Martian atmosphere. *Science* **341**, 260–263.

Weiss M. T. and Strandberg M. W. P. (1951) The microwave spectra of the deuteron-ammonias. *Phys. Rev.* **83**, 567–575.

Willetts A. and Handy N. C. (1995) The anharmonic constants for a symmetric top. *Chem. Phys. Lett.* **235**, 286–290.

Wilson, Jr., E. B. (1936) The effect of rotational distortion on the thermodynamic properties of water and other polyatomic molecules. *J. Chem. Phys.* **4**, 526–528.

Wilson E. B., Decius J. C. and Cross P. C. (1955) *Molecular Vibrations: The Theory of Infrared and Raman Vibrational Spectra*. McGraw-Hill Book Co. Press, New York.

Wolfsberg M. (1969a) Correction to the effect of anharmonicity on isotopic exchange equilibria-application to polyatomic molecules. *J. Chem. Phys.* **50**, 1484–1486.

Wolfsberg M. (1969b) Correction to the effect of anharmonicity on isotopic exchange equilibria. *Adv. Chem.* **89**, 185–191.

Wolfsberg M., Massa A. A. and Pyper J. W. (1970) Effect of vibrational anharmonicity on the isotopic self-exchange equilibria $H_2X + D_2X = 2HDX$. *J. Chem. Phys.* **53**, 3138–3146.

Woon D. E. and Dunning, Jr, T. H. (1993) Gaussian basis sets for use in correlated molecular calculations. III. The atoms aluminum through argon. *J. Chem. Phys.* **98**, 1358–1371.

Woon D. E. and Dunning, Jr, T. H. (1995) Gaussian basis sets for use in correlated molecular calculations. V. Core-valence basis sets for boron through neon. *J. Chem. Phys.* **103**, 4572–4585.

Yang S. and Liu Y. (2015) Nuclear volume effects in equilibrium stable isotope fractionations of mercury, thallium and lead. *Sci. Rep.* **5**, 12626.

Yang S. and Liu Y. (2016) Nuclear field shift effects on stable isotope fractionation: a review. *Acta. Geochim.* **35**, 227–239.

Zhang Q., Day P. N. and Truhlar D. G. (1993) The accuracy of second order perturbation theory of multiply excited vibrational energy levels and partition functions for a symmetric top molecular ion. *J. Chem. Phys.* **98**, 4948–4958.

Associate editor: James Farquhar